EURAMET TC Project
Final Report

Project Title

Interlaboratory comparison of moisture measurements with biomass samples

Coordinator, Institute, Country

Eric Georgin (LNE-CETIAT))

EURAMET Registration No.

Eric Georgin, LNE-CETIAT (France)

Subject Field

Thermometry

KCDB Identifier

--

Date

2024-04-15

EURAMET e.V., Bundesallee 100, 38116 Braunschweig, Germany
Phone: +49 531 592 1960 Fax: +49 531 592 1969 E-mail: secretariat@euramet.org
www.euramet.org

19ENG09 BIOFMET

D4: Report on traceable methods for the calibration of moisture transfer standards and reference materials

Lead Partner (D4): CETIAT

Due date of the deliverable:

30 November 2023

Actual submission date of the deliverable:

30 May 2023

Prepared by: CETIAT (lead), CMI, CTU, DTI

This publication only reflects the view of the BIOFMET Consortium or selected participants thereof. Whilst the BIOFMET Consortium has taken steps to ensure that this information is accurate, it may be out of date or incomplete, therefore, neither the BIOFMET Consortium participants nor EURAMET are liable for any use that may be made of the information contained herein. This document is published in the interest of the exchange of information and it may be copied in whole or in part providing that this disclaimer is included in every reproduction or part thereof as some of the technologies and concepts predicted in this document may be subject to protection by patent, design right or other application for protection, and all the rights of the owners are reserved. The information contained in this document may not be modified or used for any commercial purpose without prior written permission of the owners and any request for such additional permissions should be addressed to the BIOFMET coordinator.

This project 19ENG09 BIOFMET has received funding from the EMPIR programme co-financed by the Participating States and from the European Union's Horizon 2020 research and innovation programme.

EMPIR EURAMET
The EMPIR initiative is co-funded by the European Union's Horizon 2020 research and innovation programme and the EMPIR Participating States

Contents

This project 19ENG09 BIOFMET has received funding from the EMPIR programme co-financed by the Participating States and from the European Union's Horizon 2020 research and innovation programme.

The EMPIR initiative is co-funded by the European Union's Horizon 2020 research and innovation programme and the EMPIR Participating States

1 Introduction

Within the scope of this project, multiple analytical techniques are being tested to quantitatively determine the moisture content in solid biofuels, specifically wood pellets and/or wood chips. The effectiveness of these techniques is being assessed. One common characteristic among the reference methods under investigation is the application of heat to the sample to extract moisture from the solid matrix. However, this approach poses certain challenges in determining the appropriate level of heating and identifying the point at which all the moisture has been released.

In the literature, this heat treatment applied to the sample is sometimes referred to as evolved water vapor measurement techniques. Evolved water vapor measurement techniques involve quantifying and analyzing the water vapor released or evolved from a sample under specific conditions. The term "evolved" implies that the water vapor is released, generated, or liberated from the sample due to external factors or internal changes, such as temperature increase, chemical reactions, or pressure changes. These techniques aim to characterize and analyze the components of the evolved vapors. In this project, heating alone is employed, and thus evolved vapor measurement techniques involve using an oven and carrier gas to evaporate and collect the moisture from the sample.

That being said, the following reference methods have been used and studied in this project:

- Loss on drying (LoD)

The Loss on Drying (LoD) method is considered the simplest and most robust technique for moisture determination. It can be applied to a wide range of solid materials and utilizes large sample sizes. In this method, the sample is heated, causing the moisture to evaporate as vapor, and the resulting loss of mass is measured. The LoD method is widely adopted due to its simplicity and the fact that it requires only common laboratory equipment, such as an analytical balance and an oven. Industrial users often prefer this method because of its low capital expenditure (CAPEX) requirements and the minimal need for highly trained personnel.

One of the advantages of LoD is that it provides results for the entire material, giving a comprehensive picture of the moisture content. However, it should be noted that the LoD method has limited selectivity and is specifically suitable for moisture content determination.

The application of heat to the sample in LoD facilitates the release of vapors, even though LoD is not classified as an evolved water vapor technique. In LoD, the focus is on determining the change in mass resulting from the evaporation of moisture rather than analyzing the

This project 19ENG09 BIOFMET has received funding from the EMPIR programme co-financed by the Participating States and from the European Union's Horizon 2020 research and innovation programme.

released vapors. By measuring the loss in mass, the moisture content of the sample can be quantified.

- Karl Fischer titration (KF)

The Karl Fischer titration method is based on the Karl Fischer reaction and is known for its high selectivity towards water, allowing for the determination of water content instead of general moisture content. However, unlike the previous methods mentioned, this method introduces chemicals into the analysis, making the system less robust compared to the Loss on Drying (LoD) method. It also requires skilled labor to ensure reliable results. In the absence of a sample preparation module, accessing the water within the sample can be challenging, leading to increased operating costs (OPEX). Furthermore, the Karl Fischer titration equipment itself is costly. As a result of these high expenditures, this method is typically employed when other alternatives are incapable of fulfilling the required task.

Two types of Karl Fischer titration exist: volumetric and coulometric. The difference between them lies in the way the water content in a sample is quantitatively determined. Volumetric Karl Fischer titration relies on the reaction of water with a pre-determined volume of Karl Fischer reagent, while coulometric Karl Fischer titration measures the electricity needed to generate iodine consumed by the water in the sample. The choice between the two methods depends on factors such as the water content range of the sample, required accuracy, and specific application requirements.

Volumetric Karl Fischer titration is a widely used technique that relies on the reaction between the water in the sample and the Karl Fischer reagent. The reagent consists of an iodine solution, sulfur dioxide, pyridine, and a solvent. In this method, a known volume of the Karl Fischer reagent is added to the sample containing water. The iodine reacts with water, and the endpoint of the titration is determined by the color change of the solution using a visual indicator or automated detection. The amount of water in the sample is calculated based on the volume of the reagent consumed.

On the other hand, coulometric Karl Fischer titration is an electrochemical method for determining water content. This technique involves the generation of iodine through an electrochemical reaction. The iodine is then consumed by the water in the sample. The amount of electricity required to produce the necessary iodine is directly proportional to the water content in the sample. By measuring the electrical current during the titration, the water content can be quantified. Coulometric Karl Fischer titration is often preferred for samples with very low water content or when higher accuracy is required.

This project 19ENG09 BIOFMET has received funding from the EMPIR programme co-financed by the Participating States and from the European Union's Horizon 2020 research and innovation programme.

The EMPIR initiative is co-funded by the European Union's Horizon 2020 research and innovation programme and the EMPIR Participating States

Coulometric Karl Fischer titration can be utilized as part of the evolved water vapor technique by combining it with an oven and carrier gas. This setup allows for the evaporation and collection of moisture from the sample, which is then directed to the electrochemical reactor. Thus, in this case, this measurement technique can be classified as evolved water vapor coulometry analysis.

- Evolved Water Vapour coulometric analysis

Here, evolved vapor coulometry analysis relies on the selective electrolysis of evaporated water from a solid matrix, carried in a stream of carrier gas.

The process involves heating the sample in an oven to evaporate the moisture, followed by the reaction of water molecules with a P_2O_5 coating, resulting in the formation of H_3PO_4. Within the electrolytic cell, H_3PO_4 molecules dissociate into hydrogen and oxygen. The electric charge consumed during electrolysis is measured over time and integrated to determine the total charge, which is directly proportional to the amount of water in the sample according to Faraday's law. Consequently, water molecules are selectively electrolyzed, and the current passing through the cell corresponds to the quantity of water present.

This technique enables the differentiation between different forms of water bonding, such as free water and chemically bound water. Electrolysis of H_3PO_4 is commonly utilized for measuring low levels of moisture, typically below approximately 10%. Faraday's law plays a crucial role in this method as it describes the relationship between the amount of electric charge passed through an electrochemical cell and the quantity of material dissolved at the electrodes. In this approach, Faraday's law is applied to determine the water content in the sample based on the electric charge passed through the cell during the electrolysis process.

- Evolved Water Vapour dew-point analysis

In this technique, an oven and a water-selective sensor are utilized, leading to its classification as evolved water vapor analysis. The sensor is specifically designed to be selective towards water, enabling the analysis of water content in solids. Similar to LoD, the heating stage facilitates the release of water from within the sample. The water vapor is then condensed on a chilled mirror to determine the dew/frost point temperature. The quantity of water is correlated with factors such as gas flow, gas pressure, and dew/frost point temperature. This technique offers detection limits comparable to Karl Fischer titration but without the use of hazardous chemicals required in the latter.

This project 19ENG09 BIOFMET has received funding from the EMPIR programme co-financed by the Participating States and from the European Union's Horizon 2020 research and innovation programme.

Reference methods typically offer the highest accuracy and the lowest uncertainties. However, they often rely on equipment that operates under laboratory conditions, which can pose challenges when it comes to ensuring traceability to the International System of Units (SI) for instruments installed in industrial sites where removal is not feasible. To address this issue, transfer standards have been developed as part of this project. These standards have been calibrated using one of the reference methods mentioned earlier, ensuring their traceability and reliability in industrial settings.

2 Reference methods and transfer instruments used in this project

2.1 Reference methods

2.1.1 Loss on drying

2.1.1.1 General overview

Loss on drying is a thermos-gravimetric technique, it operates on the principle that when a material is heated, moisture is extracted from it. The moisture content is determined by measuring the difference in mass before and after heating. This method is based on the assumption that the loss in mass is primarily caused by the evaporation of water and other volatile components from the sample. However, it's important to note that the measured value can be highly dependent on the predefined temperature and heating time used in the method.

Two commonly used techniques for moisture determination are loss on drying and moisture balance, also known as a moisture analyzer. In the literature, results can be presented in both wet and dry basis. Both representations indicate the moisture content, but there is a distinction. Wet basis refers to the result being relative to the mass of the wet sample, while dry basis refers to the result being relative to the residual mass (or in other words, the mass of the dry sample).

$$Moisture\ Content_{wet\ basis} = \frac{m_{wet.sample}(g) - m_{dry.sample}(g)}{m_{wet.sample}(g) - m_{container}(g)} \times 100 \quad (1)$$

Where: $m_{container}$ – *mass of the empty sample container,* $m_{wet.sample}$ – *mass of the sample container plus the wet sample,* $m_{dry.sample}$ – *mass of the sample container plus the dry sample (after heating).*

$$Moisture\ Content_{dry\ basis} = \frac{m_{wet.sample}(g) - m_{dry.sample}(g)}{m_{dry.sample}(g) - m_{container}(g)} \times 100 \quad (2)$$

This project 19ENG09 BIOFMET has received funding from the EMPIR programme co-financed by the Participating States and from the European Union's Horizon 2020 research and innovation programme.

Where: $m_{container}$ – *mass of the empty sample container,* $m_{wet.sample}$ – *mass of the sample container plus the wet sample,* $m_{dry.sample}$ – *mass of the sample container plus the dry sample (after heating).*

An example of measuring steps is described below:

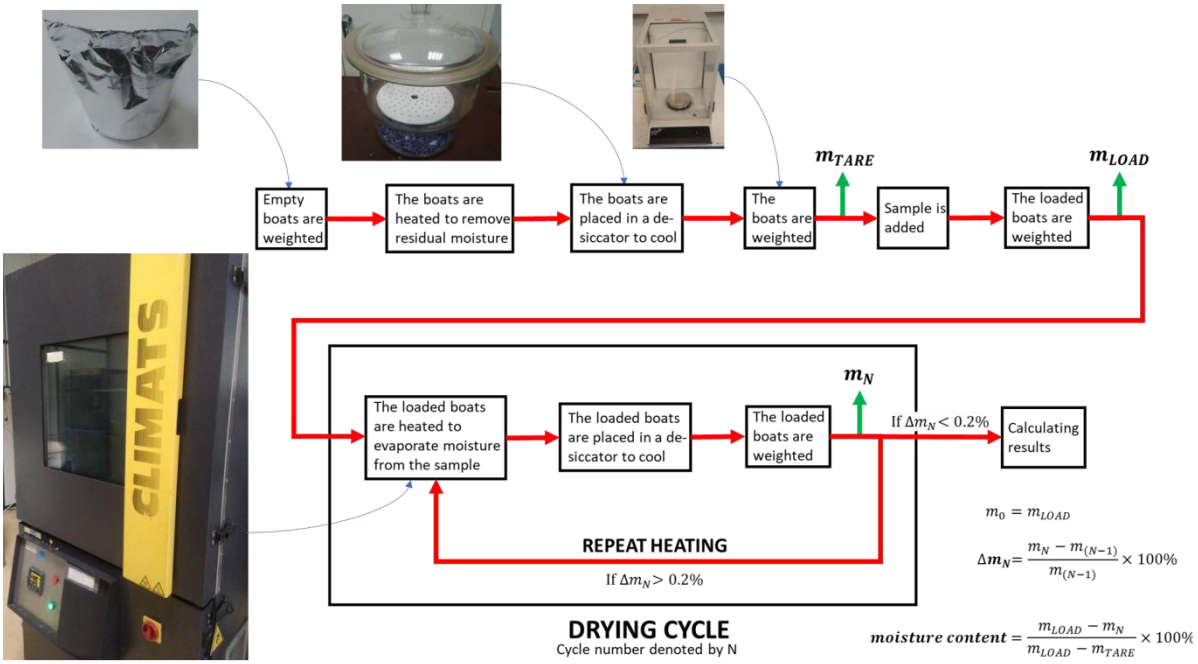

Figure 1 LoD measuring steps

In the Figure 1, it can be observed that the cooling step in a desiccator before weighing the loaded boat may deviate from the standards outlined in EN ISO 18134:2015. The standard specifies that weighing should be conducted while the sample holder is still hot, using thermal insulation to prevent any impact on the scale during weighing. This approach offers the advantage of preventing re-absorption of water from the air into the sample.

However, when a cooling step is introduced, it is performed inside a desiccator to avoid re-absorption of water from the air into the sample. The weighing is conducted when the boat is cold, resulting in the cancellation of natural convection movements of air. This is particularly important for accurate determination, especially when dealing with small quantities of the sample

The two quantities are liked thanks to the following equations

$$M.C._{d.b.} = \frac{M.C._{w.b.}}{1 - M.C._{w.b.}} \text{ and } M.C._{w.b.} = \frac{M.C._{d.b.}}{1 + M.C._{d.b.}} \quad (3)$$

This project 19ENG09 BIOFMET has received funding from the EMPIR programme co-financed by the Participating States and from the European Union's Horizon 2020 research and innovation programme.

Loss on drying one of the most widely-used and oldest methods for the determination of moisture in solid material. This method is described in the series of standard EN ISO 18134-1:2015, 18134-2:2015, and 18134-3:2015, which replace the series of standard EN ISO 14774-1:2009, 14774-2:2009, and 14774-3:2009. Comparing to the measuring steps proposed just above the following point should be considered:

- The mass sample to be analyzed
- The mass per square centimeter of the sample in the tray
- The drying temperature, typically 105 °C ± 2 °C
- Dryness of the sample : 0,2 % variation of the initial mass of the sample
- The weighing, within 10 or 15 seconds after the drying, while the sample is still hot
- The drying time lower than 24 h

2.1.1.2 In use within the project

Two methods for loss on drying have been used throughout the project: the first one described in the standard and the second one derived from EWV-dew-point analysis.

The standardized method, described in EN ISO 18134:2015, is used independently. In this method, samples weighing approximately 200 g are placed in an aluminum tray, weighed, and placed in an oven for drying at 105 °C ± 2 °C for a maximum of 24 hours.

To estimate the moisture content in the material, the sample is weighed after drying is complete, and the mass change is calculated. To ensure that the sample is thoroughly dried, an additional measurement is conducted after an extra hour of drying. The difference between the two measurements must not exceed 0.2% of the mass change. For example, if a mass change of 30 g is observed between the wet sample and the first weighing, the second weighing must not deviate by more than 0.06 g.

The post-drying weighing is performed while the sample is still warm to prevent re-absorption of water from the air into the sample, which could occur if the sample were allowed to cool down first.

In addition to the loss on drying method described above, a second method for loss on drying is performed in parallel with the "EWV - dew point hygrometer" method. This method is referred to as "EWV-LoD" in the report. The experimental facility developed allows for the measurement of water content using the "EWV - dew point hygrometer" analysis or the measurement of loss on drying by comparing the mass before and after the "EWV - dew point hygrometer" analysis. This serves as a practical sanity check to ensure that the water content

This project 19ENG09 BIOFMET has received funding from the EMPIR programme co-financed by the Participating States and from the European Union's Horizon 2020 research and innovation programme.

obtained from the EWV method does not exceed the measured mass loss using the EWV-LoD method.

In the EWV-LoD method, the sample is placed in a container and sealed using valves. The chamber with the sample is weighed on a comparator. The chamber is then placed in an oven and connected to a supply of dry gas. The oven is turned on, and the valves are opened, allowing the dry gas to pass through the sample. As the sample is slowly heated up to a maximum temperature of 105 °C, the water in the sample evaporates into the dry gas, humidifying it. The aim is to maintain a dew point of 50 °C ± 2 °C at the dew point hygrometer. Once the sample is dry, the dew point of the humidified gas decreases, and when it reaches below a limit of -15 °C, the drying procedure is complete. The valves on both sides of the chamber are then closed, and the chamber is allowed to cool down.

Once the chamber has cooled, it is measured again, and the mass difference is determined to calculate the loss on drying.

2.1.1.3 Uncertainties

The main uncertainty components for the loss on drying methods are

- Mass of the tray
  - Scale: Calibration, Drift, Resolution, Calibration modelling, Repeatability Eccentricity, Environment,
  - Measurements : Experimental measurements
  - Tray : Archimedes buoyancy,
- Initial total mass of the sample
  - Scale: Calibration, Drift, Resolution, Calibration modelling, Repeatability Eccentricity, Environment,
  - Measurements : Experimental measurements
  - Tray : Archimedes buoyancy,
- Final total mass
  - Scale: Calibration, Drift, Resolution, Calibration modelling, Repeatability Eccentricity, Environment,
  - Measurements : Experimental measurements
  - Tray : Archimedes buoyancy

The typical uncertainty achieved at LNE-CETIAT with wood pellets is presented in the table below:

This project 19ENG09 BIOFMET has received funding from the EMPIR programme co-financed by the Participating States and from the European Union's Horizon 2020 research and innovation programme.

	Quantification	Unit	Standard Uncertainty	Sensitivity coefficient	$(\partial y/\partial x_i)^2 \cdot u^2(x_i)$
Initial mass	0,017	g	0,0085	4,68E+00	1,59E-03
Final mass	0,049	g	0,0246	-4,98E+00	1,49E-02
Mass of the tray	0,0110	g	0,0055	3,01E-01	2,76E-06

résultat =	6,04	g/100 g
$U_{k=2}$ =	0,26	g/100 g

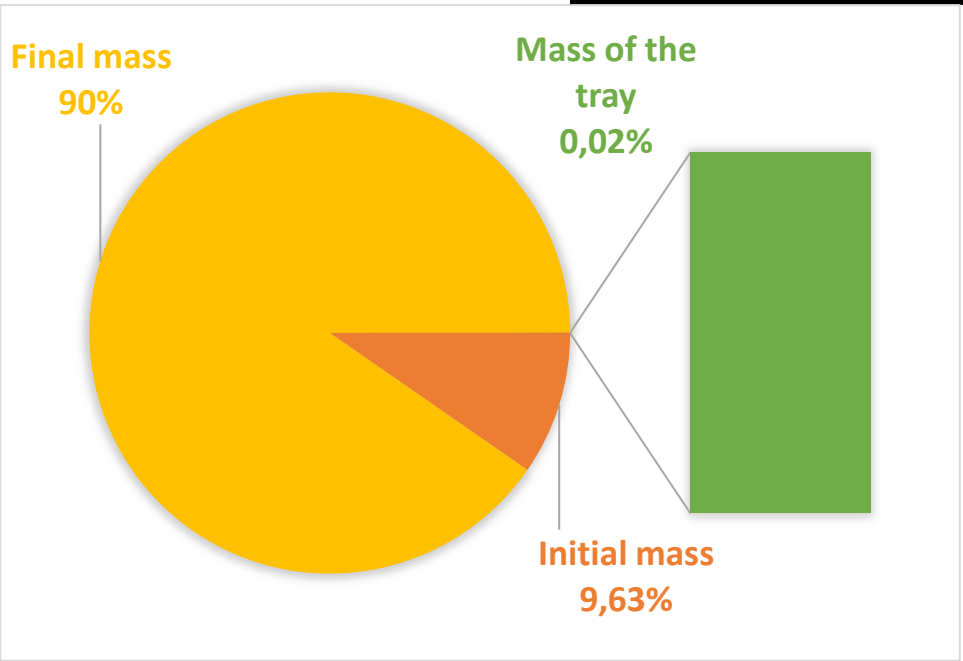

Figure 2 uncertainties of LoD

2.1.2 Coulometric Karl-Fischer titration

2.1.2.1 General overview

Karl Fischer titration (KF) is dedicated to water content measurement. It was originally conceived as a volumetric titration method with visual determination of the end-point. The method is based on the Karl Fischer reaction, discovered in 1935 by a German chemist, from whom it derives its name [6]. In the KF reaction, a single molecule of iodine is consumed by each water molecule. The strict stoichiometry of this method allows for the quantification of the amount of water through knowing the amount of iodine consumed.

I stage
$$ROH + SO_2 + R'N \rightarrow [R'NH]SO_3R \quad (4)$$

II stage
$$[R'NH]SO_3R + H_2O + I_2 + 2 \times R'N \rightarrow 2 \times [R'NH]I + [R'NH]SO_4R \quad (5)$$

Two complementary KF titration methods are in widespread use: volumetric (vKF) and coulometric (cKF). The reagents used with volumetric systems are divided in to two groups:

This project 19ENG09 BIOFMET has received funding from the EMPIR programme co-financed by the Participating States and from the European Union's Horizon 2020 research and innovation programme.

one- and two-component reagents. One-component reagents contain all the necessary reactants in one solution, the titrant. Their titer is less stable and therefore it has to be re-determined more often. However, this is offset by their ease of use – they offer more flexibility in terms of solvents for dissolving the sample [7]. The vKF method is used for samples with water content between 1 % and 100 %.

The cKF method differs in the way iodine is introduced in to the reaction medium – the iodine necessary for the reaction is electrochemically generated in the measurement cell from iodide ions already present in the reagent. Compared to the vKF method, cKF offers better accuracy of measuring the amount of iodine. This is possible, because the amount of generated iodine is proportional to the consumed coulombs through Faradays law. On the other hand, the maximum speed of generating iodide is limited by the system and therefore it is unsuitable for the determination of large quantities of water. As a result, cKF is suitable for the determination of trace amounts of water, from a few ppm to few %.

In its original setup, KF suffered from poor reliability associated with end-point determination. This was based on the excess of iodine, which colours the titration media yellow. However, the reproducible determination of this moment is difficult as samples can affect the colour of the media, the colour does not change rapidly and it depends on the used solvent. It required a very experienced analyst. Modern instruments use electrochemical methods for reliable and accurate end-point determination, most often voltametric technique as it provides more accurate results [8].

The most common way of sample introduction in KF is by injecting the sample directly into the measurement cell with a syringe. This necessitates the dissolving of solid sample, which is costly in time and money. For analysing solid sample, specialized sampling systems have been introduced and made commercially available. The work by heating the sample and then carrying the evolved water vapour to the titration cell with a stream of dried carrier gas. Whilst it makes the overall system more complex, it makes the analysis of solid samples much faster.

Because the sample is not introduced directly into the titration medium, its lifetime is increased, thus reducing unnecessary waste.

The 899 KF Coulometer (Metrohm AG, Switzerland) coulometric titrator was used for Karl Fischer titration. Resolution is specified as 1 µg of water. For analysing solid samples, the titrator was combined with 860 KF Thermoprep (Metrohm AG, Switzerland), for thermal sample preparation in Karl Fischer titration. Both instruments were operated via a computer running Tiamo 2.4 full software (Metrohm AG, Switzerland).The generator electrode used had a diaphragm. The anolyte, HYDRANAL Coulomat AG Oil and the catholyte, HYDRANAL Coulomat CG, were both sourced from Sigma-Aldrich, United States (now part of Merck KGaA, Germany).

This project 19ENG09 BIOFMET has received funding from the EMPIR programme co-financed by the Participating States and from the European Union's Horizon 2020 research and innovation programme.

Figure 3 899 KF + 860 KF Thermoprep for oven coulometric Karl Fisher titration – O-cKF or Evolved Water Vapour coulometric Karl Fischer titration

Before performing any work, the system is allowed to stabilize – assessed by monitoring the speed at which the water is titrated at standby. This system uses closable vials instead of open boats. Therefore, a larger number of samples can be prepared at one time. A number of vials are closed without adding a sample – blank vials. Into the rest of vials, samples are weighted and then closed. The vials are then loaded on the sample rack and the analysis sequence is started. The optimal amount of water per sample, for the O-cKF, is approximately 1000 µg. A benefit of having a large volume of very dry reagent in the measurement cell is that the reagent can absorb a significant quantity of water.

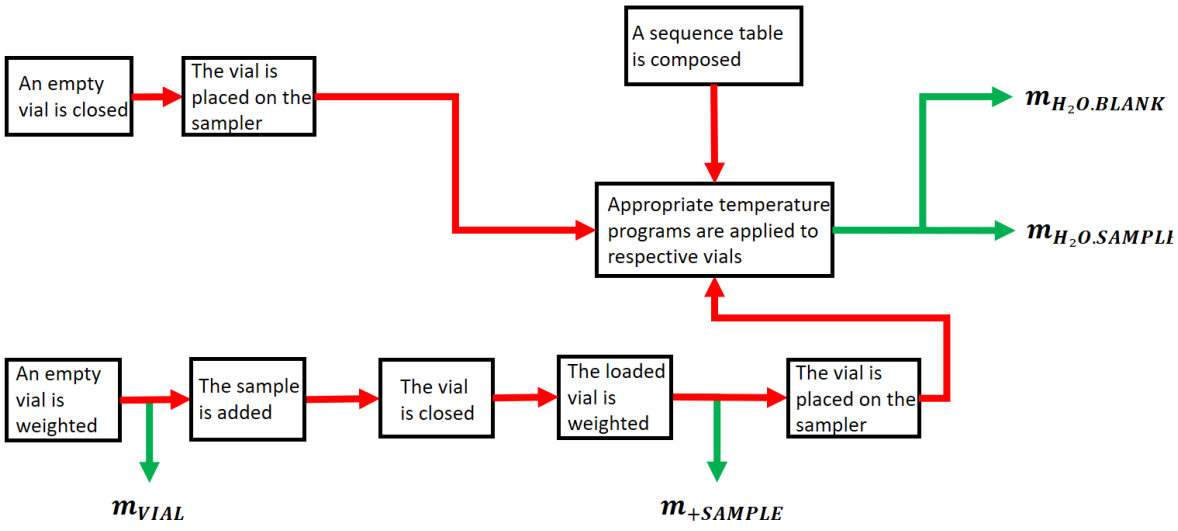

$$\textbf{water content of the sample} = \frac{m_{H_2O.SAMPLE} - m_{H_2O.BLANK}}{m_{+SAMPLE} - m_{VIAL}} \times 100\%$$

Figure 4 Schematic representation of the measurement process with the EWV instrument [1]

This project 19ENG09 BIOFMET has received funding from the EMPIR programme co-financed by the Participating States and from the European Union's Horizon 2020 research and innovation programme.

2.1.2.2 *Uncertainties*

The main uncertainty components are

- Mass of the sample
  - Scale: Calibration, Drift, Resolution, Calibration modeling, Repeatability Eccentricity, Environment,
  - Measurements : Experimental measurements
  - Tray : Archimedes buoyancy,
- Tare determination
- Water content measurement
  - Repeatability, reproducibility, bias

The typical uncertainty achieved at LNE-CETIAT with wood pellets is presented in the table below:

	Quantification	Unit	Standard Uncertainty	Sensitivity coefficient	$(\partial y/\partial x_i)^2 \cdot u^2(x_i)$
Mass of water in the sample	8,429	µg	4,2144	4,99E-03	4,43E-04
Tare	7,691	µg	3,8453	-4,99E-03	3,68E-04
Sample mass	0,0004	g	0,0002	-3,57E+02	4,75E-03

résultat =	7,16	g/100 g
$U_{k=2}$ =	0,15	g/100 g

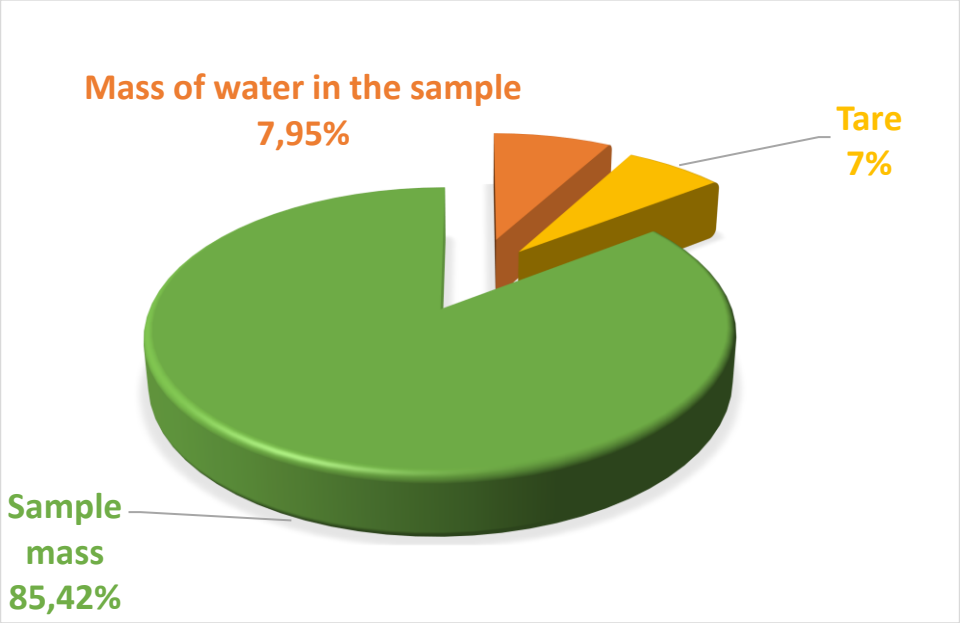

Figure 5 uncertainties of O-cKF or Evolved Water Vapour coulometric Karl Fischer titration

This project 19ENG09 BIOFMET has received funding from the EMPIR programme co-financed by the Participating States and from the European Union's Horizon 2020 research and innovation programme.

2.1.3 Evolved water vapour dew-point analysis

2.1.3.1 General overview

Danish Technological Institute utilizes a method for determining moisture content, which is based on evaporating the water into a dry gas-stream and leading this gas-stream past a dew point hygrometer and a capacitive humidity sensor.

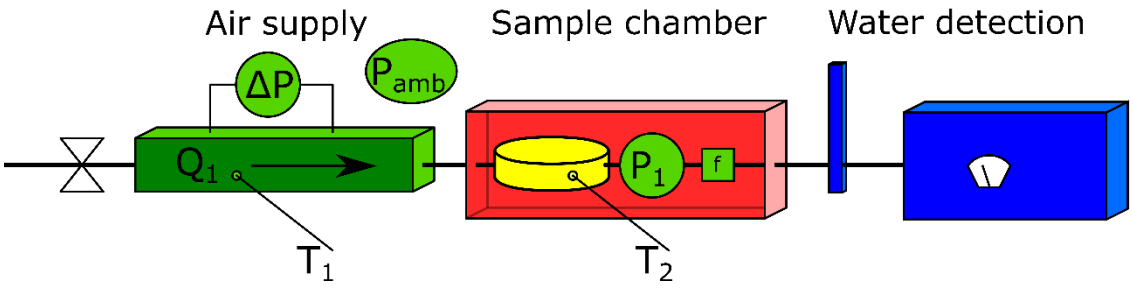

Figure 6: Evolved water vapour dew-point analysis-setup at DTI. Dry air enters from the left, water is extracted from the sample in the yellow chamber, and the wet air is measured at the dew point sensors to the right.

The set-up, seen in Figure 4, consists of a sample chamber with two valves. The sample is placed within the sample chamber, a lid is placed on top, and the valves are closed.

The chamber, including the sample, is installed in an oven, and connected to a flow of dry nitrogen gas. The valves are opened, and the oven is turned on. The sample will evaporate its water into the nitrogen, and the gas is transported, through a heated pipe, to a dew point hygrometer. The temperature of the oven is controlled to yield a dew point of 50 °C at the dew point hygrometer. To compensate for any potential pollution of the dew point hygrometer (residues on the mirror), a mirror check is performed every 30 minutes.

Once the sample starts drying, and the temperature of the oven has reached its pre-defined final temperature of 105 °C, the dew point, measured at the dew point hygrometer, will start to drop. When this has reached a certain lower limit of -15 °C, the sample is considered dry, and the oven will shut down. The valves of the sample chamber are closed, and the sample chamber can be cooled down and measured to find the weight loss of the sample during the drying process.

Water content of the sample is found by fitting the relative humidity sensor to the dew point hygrometer after each mirror cleaning. The fitted data from the relative humidity sensor is transformed into the absolute water content of the air, using Hardy [9]. This gives the amount of water per volume of gas. Multiplying the absolute water content with the air flow, measured at the LFE, gives the amount of water leaving the sample chamber at any given time. By integrating this measure over the duration of the drying period, the total amount of water having left the sample is found.

This project 19ENG09 BIOFMET has received funding from the EMPIR programme co-financed by the Participating States and from the European Union's Horizon 2020 research and innovation programme.

EMPIR EURAMET
The EMPIR initiative is co-funded by the European Union's Horizon 2020 research and innovation programme and the EMPIR Participating States

All the measurements used for calculating the flow rate and the absolute water content are adjusted based on pressure and temperature, which are measured continuously.

2.1.3.2 Uncertainties

The main uncertainty components are

- Measurement of gas flow through laminar flow element
  - Measurement of differential pressure
  - Measurement of gas viscosity
- Measurement of dew point
- Fit of capacitive sensor to dew point hygrometer

A detailed uncertainty budget for the EWV + dew point hygrometer is seen in Appendix 1, and a detailed description of the setup, including descriptions of the specific equipment used is found in Østergaard & Nielsen [11].

During an optimal run, an uncertainty of 1.4 % moisture content can be obtained, however most often, the actual uncertainty will not be better than 2.0 %.

2.1.4 Evolved Water Vapour coulometric analysis

2.1.4.1 General overview

Coulometry is based on the measurement of the amount of electricity consumed or produced and deriving from it the amount of matter transformed. The techniques are divided in to two categories: potentiostatic and amperostatic. In the former the potential is kept constant and the change in current is measured. In the case of the latter, it is the other way around. The determination of water through the use of coulometry has evolved in to two methods: coulometric Karl Fischer titration, presented before, and water-selective sensors.

The most common form of the water-selective sensors relies on the extremely hygroscopic nature of anhydrous P_2O_5. At first it was used as a desiccant, but the hydrolysis products forming on its' surface hamper the reactivity. To circumvent this, electrolytic regeneration was introduced in 1933 [2]. This invention paved the way for the first devices, introduced around 1960, intended for the direct measurement of water in gases via coulometry [3], [4]. According to Faradays' law, the amount of water electrolysed is equal to the consumed current. The sensor's design incorporates an electrode, printed on an Al_2O_3 support, enabling faster production and higher quality. Furthermore, the wet gas flow is distributed over the entire sensor surface, yielding a more even load and resulting in better reliability.

This project 19ENG09 BIOFMET has received funding from the EMPIR programme co-financed by the Participating States and from the European Union's Horizon 2020 research and innovation programme.

$$m = \frac{M \times \int i(t)dt}{Z \times F}$$

m – mass of water;
M – molar mass (water: 18.016 g/mol)
i(t)dt – electrical charge per time
Z – number of released electrons (2)
F – Faradays constant (96484.56 C/mol)

Faraday's law [1]

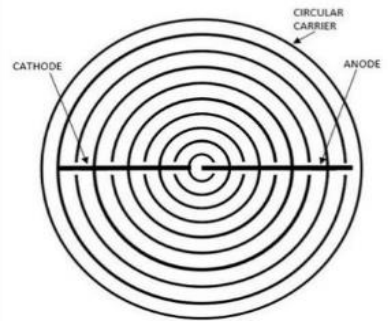

P_2O_5 sensor [1]

Figure 7

The process involves heating the sample in an oven to evaporate the moisture, followed by the reaction of water molecules with a P_2O_5 coating, resulting in the formation of H_3PO_4. Within the electrolytic cell, H_3PO_4 molecules dissociate into hydrogen and oxygen. The electric charge consumed during electrolysis is measured over time and integrated to determine the total charge, which is directly proportional to the amount of water in the sample according to Faraday's law. Consequently, water molecules are selectively electrolyzed, and the current passing through the cell corresponds to the quantity of water present.

This sensor was used to develop a device, easyH_2O, Berghof Products + Instruments GmbH, Eningen, Germany, for the determination of trace water content in solid samples. This instrument is composed of the following parts:

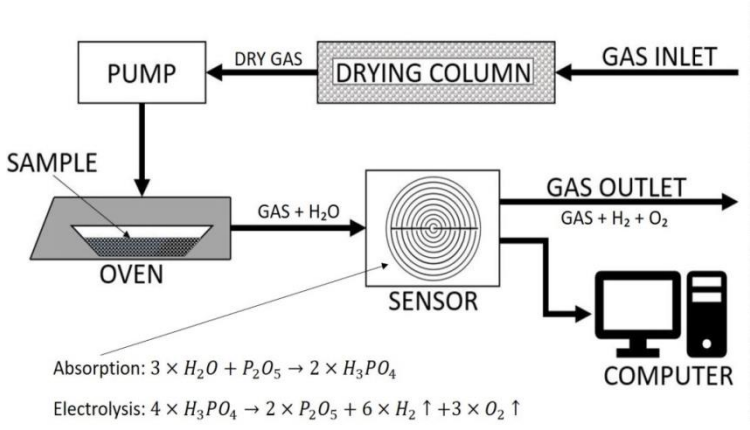

1. Drying column to dry the carrier gas.
2. Pump for the carrier gas.
3. Oven to heat the sample.
4. Sensor to detect the presence of water.

Figure 8 EWV instrument [1], [5]

This project 19ENG09 BIOFMET has received funding from the EMPIR programme co-financed by the Participating States and from the European Union's Horizon 2020 research and innovation programme.

The system is controlled and the data is registered by proprietary Aqualys software (Berghof). The results are displayed on a graph in real time. The program allows to apply different temperature profiles in the range of ambient temperature to 400 °C, in order to study the evolution of water from the sample as a function of temperature. For reference measurements, a solid certified reference material with 1 g/100g water content was used.

For obtaining reliable results, it is paramount that the background current is as stable as possible. This estimated from the tare measurements and the displayed current value on standby. The samples are analysed in special boats. The sample is weighted in to them before inserting the boat in the oven. The desired sample size optimised, keeping in mind the performance of the analytical balance, the sample must be at least 10 mg in our case, and the total amount of water per sample, preferably around 200 µg in our case. Larger amounts of water will lead to sensor saturation, giving biased results; unreasonably long analysis times and also decrease the interval between sensor regeneration. Then the analysis is started by applying the temperature program.

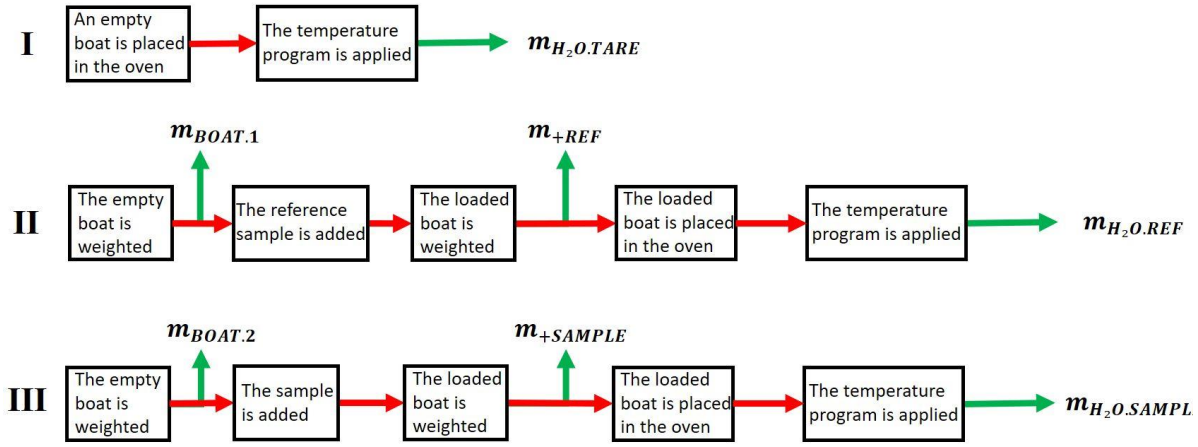

$$\textbf{water content of the sample} = \frac{reference\ sample\ value\ (\%)}{\frac{m_{H_2O.REF} - m_{H_2O.TARE}}{m_{+REF} - m_{BOAT.1}} \times 100\%} \times \frac{m_{H_2O.SAMPLE} - m_{H_2O.TARE}}{m_{+SAMPLE} - m_{BOAT.2}} \times 100\%$$

Figure 9 Schematic representation of the measurement process with the EWV instrument [1]

The temperature program is optimized for each type of sample separately during the method development phase. By changing the duration, temperature and heating speed, it is possible to differentiate between different water binding forms. In some cases, it allows to control the release of water from the sample, as not to saturate the sensors. If it would occur, some part of the water released from the sample would be left undetected and in turn incur a bias.

This project 19ENG09 BIOFMET has received funding from the EMPIR programme co-financed by the Participating States and from the European Union's Horizon 2020 research and innovation programme.

2.1.4.2 *Uncertainties*

The main uncertainty components are

- Mass of the sample
  - Scale: Calibration, Drift, Resolution, Calibration modelling, Repeatability Eccentricity, Environment,
  - Measurements : Experimental measurements
  - Tray : Archimedes buoyancy,
- Tare determination
- Water content measurement
  - Repeatability, reproducibility, bias

The typical uncertainty achieved at LNE-CETIAT with wood pellets is presented in the table below:

	Quantification	Unit	Standard Uncertainty	Sensitivity coefficient	$(\partial y/\partial x_i)^2 \cdot u^2(x_i)$
Mass of water in the sample	22,303	µg	11,1513	4,97E-03	3,07E-03
Tare	18,271	µg	9,1353	-4,97E-03	2,06E-03
Sample mass	0,0002	g	0,0001	-3,01E+02	8,30E-04

résultat =	7,12	g/100 g
$U_{k=2}$ =	0,15	g/100 g

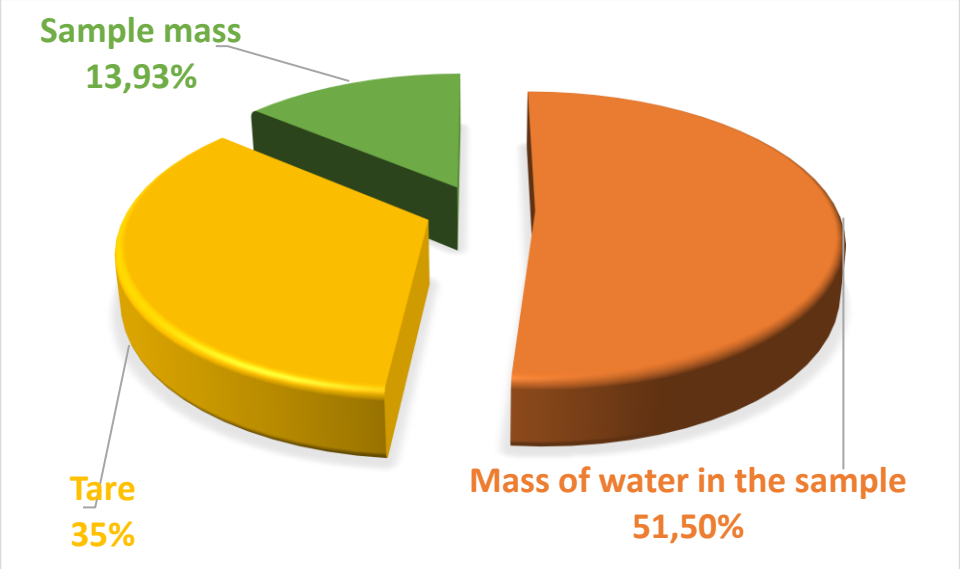

Figure 10 uncertainties of O-cKF or Evolved Water Vapour coulometric Karl Fischer titration

This project 19ENG09 BIOFMET has received funding from the EMPIR programme co-financed by the Participating States and from the European Union's Horizon 2020 research and innovation programme.

2.2 Transfer instruments

2.2.1 Electromagnetic Resonant Cavity

2.2.1.1 Fundamental theory of the Cavity Perturbation method (CPM)

Several resonance methods have been developed to measure the dielectric properties of materials in recent decades. Within the framework of this project, *LNE-CETIAT* and *Fresnel Institute* have developed a resonant cavity using microwaves and based on the perturbation induced on the resonance frequency of a cavity.

The developed cavity is a closed stainless steel hollow cylinder with a cyndrical sample holder set in the central part. The method used in this work is based on the Cavity Perturbation Method (CPM). It relies on a comparative analysis of electromagnetic properties between the empty cavity and the partially loaded cavity with the sample to be analyzed. The hypothesis of the CPM is that the electromagnetic fields, inside the cavity, is affected by the introduction of a material. Thus, small variation of the EM field between empty cavity and loaded cavity can be observed.

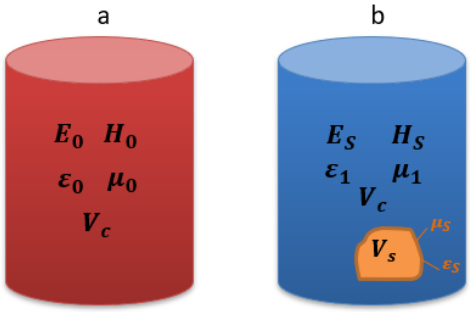

Figure 11 Schematic view of CPM, a) empty cavity and b) loaded cavity

Where

$\mathbf{E_1}$: electric field in the empty cavity; $\mathbf{E_2}$: electric field in the perturbed cavity; $\mathbf{H_1}$: magnetic field in the empty cavity; $\mathbf{H_2}$:magnetic field in the perturbed cavity; $\boldsymbol{\varepsilon_1}$: permittivity of the empty cavity; $\boldsymbol{\varepsilon_2}$: permittivity of the sample; $\boldsymbol{\mu_1}$: permeability of the empty cavity; $\boldsymbol{\mu_2}$: permeability of the sample; $\mathbf{V_c}$: cavity volume; $\mathbf{V_s}$: sample volume

By using the Maxwell equations for the empty and perturbed cavities, the analytical expressions for the real and imaginary part of the complex dielectric permittivity, the resonance frequency shift and the change in quality factor Q leads to:

$$2\left(\frac{f_0 - f_s}{f_s}\right) = (\varepsilon_r' - 1)C \qquad 6$$

$$\frac{1}{Q_s} - \frac{1}{Q_0} = \varepsilon_r'' C \qquad 7$$

This project 19ENG09 BIOFMET has received funding from the EMPIR programme co-financed by the Participating States and from the European Union's Horizon 2020 research and innovation programme.

C is the calibration constant that depends on the cavity volume, sample volume, and the electric fields in the empty cavity and the cavity filled with material. This parameter is mathematically represented by the following equation:

$$C = \frac{\iiint_{V_s} (E_s . E_0) dV}{\iiint_{V_c} (|E_0|^2) dV} \quad (8)$$

This constant, which is required for calculating the dielectric permittivity of the material under test, can be determined experimentally by a separate experiment using reference materials with known permittivity. Once this parameter is calculated, we can now measure the permittivity of an unknown material.

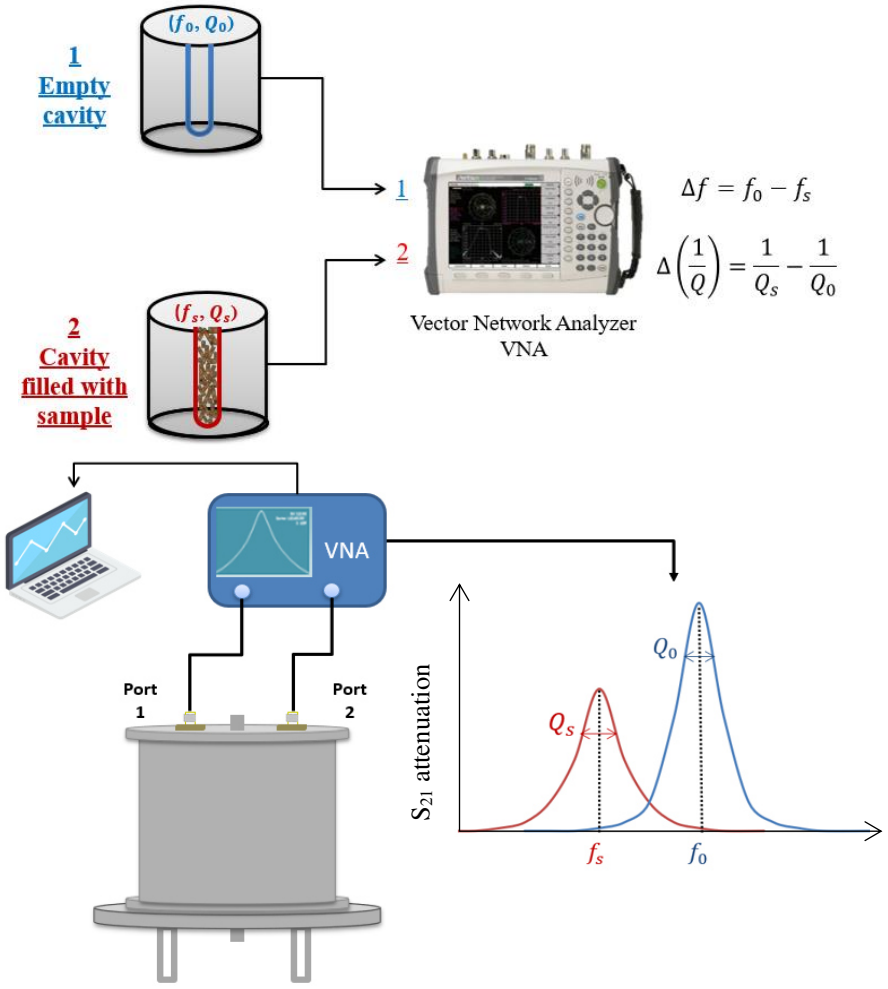

Figure 12 Measuring principle of the resonant cavity

This project 19ENG09 BIOFMET has received funding from the EMPIR programme co-financed by the Participating States and from the European Union's Horizon 2020 research and innovation programme.

2.2.1.2 Experimental set up

The system developed is a stainless steel cylinder with a diameter of 213 mm and a height of 185 mm. The electromagnetic field inside the cavity is excited via two antennas placed on the upper cavity side. The sample holder, placed in the center of the cavity, is a glass tube with an inside diameter of 36 mm and almost the same length of the cavity (internal volume about 188,35 cm^3). This system is connected to a vector network analyser that measures the attenuation (S_{21} parameter) inside the cavity. From this parameter, we can deduce the resonance frequency and the quality factor of the cavity.

Figure 13 Pictures of the resonant cavity

2.2.1.3 Numerical simulation

Numerical simulations have been performed using the HFFS software, in order to define the final design of the measurement system. Moreover, in order to facilitate the experimental work and to obtain better performance by using the perturbation technique, a comparison between the numerical results obtained with HFFS (Software for EM modeling and simulation) and the experimental results have been done. Within several possible alternative experimental configurations, the combination of mounting two straight probes (length 30 mm, inner diameter 1,2 mm and outer diameter 3,5 mm) on the upper cavity side, the selection of the well isolated mode TM_{010} within the microwave spectrum, and the positioning of a glass tube sample holder (outer diameter 40,5 mm; thickness 3,4 mm) in the center, was found to be a convenient choice, driven by the results of preliminary FEM simulations of the small perturbation induced by the insertion of the sample holder onto mode TM_{010} eigenfrequency.

This project 19ENG09 BIOFMET has received funding from the EMPIR programme co-financed by the Participating States and from the European Union's Horizon 2020 research and innovation programme.

EMPIR EURAMET
The EMPIR initiative is co-funded by the European Union's Horizon 2020 research and innovation programme and the EMPIR Participating States

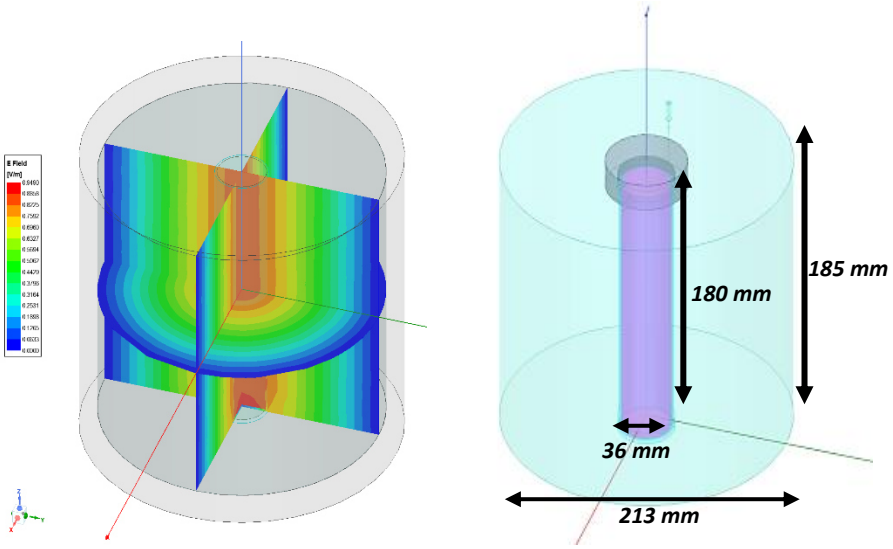

Figure 14 (Left) 3D representation of the EM field in of the cavity with the presence of glass tube in the center of the cavity, for TM010. (Right) Physical dimensions of the cavity

A comparison between numerical simulation and experimental results is presented below. It shows the relative good agreement between the numerical spectrum and the experimental spectrum of the resonant cavity.

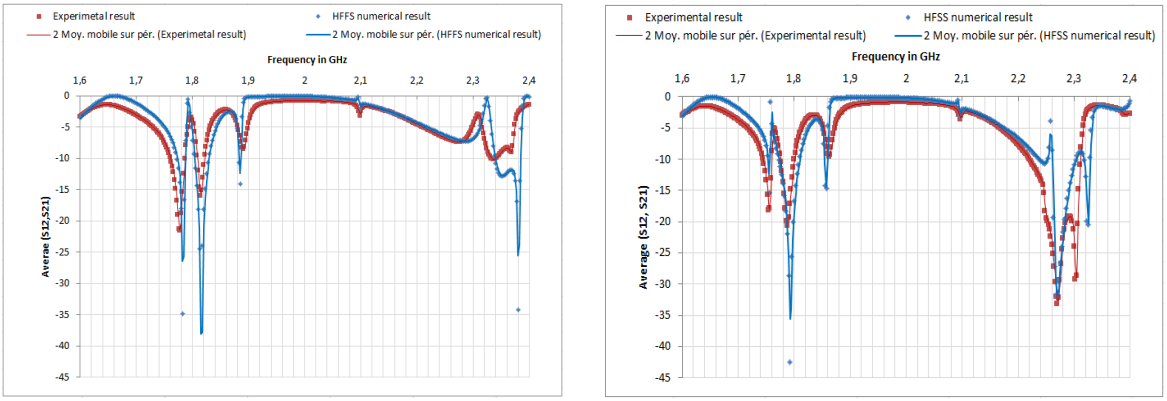

Figure 15 Microwave spectrum comparison between numerical and experimental results: (left) for empty cavity, (right) for tube filled with Teflon

When the resonant cavity is empty (considered as simply filled with air) at ambient temperature, with the glass tube inserted vertically in the center of the cavity, the frequency f_0 , corresponding to TM_{010} resonance frequency, is about 2,32 GHz. This frequency shifts to 2,26 GHz by filling the cavity with Teflon.

This project 19ENG09 BIOFMET has received funding from the EMPIR programme co-financed by the Participating States and from the European Union's Horizon 2020 research and innovation programme.

2.2.2 Acoustic Resonant Cavity

2.2.2.1 Acoustic resonance frequency of cylindrical cavity and its relation to the temperature and humidity

The natural acoustic modes of a hollow cylindrical cavity are derived e.g., in [11], as

$$f_{l,m,n} = \frac{u}{2\pi}\left[\xi_{l,m}^2 + \frac{n\pi^2}{D}\right]^{\frac{1}{2}}, \qquad (1)$$

where *l*,*m*,*n* are integers ≥ 0, *u* denotes the speed of sound inside the cavity, *D* is the diameter of a cylinder and $\xi_{l,m}$ is obtained by dividing the stated values of $\xi_{l,m}R$ in Table 1 [11] by the radius of the cavity *R*.

Table 1: Cylindrical cavity natural circular wavenumbers as given in [11]

m	0	±1	2	3
l = 0	-	0	0	0
l = 1	1.2556	2.4048	3.5180	4.6123
l = 2	4.0793	5.5201	6.8661	8.1576

Derivation of eigenfrequencies of finite length circular cylindrical shells in the axial direction can be found in [12] and corresponding axial resonance frequencies can be written in the form of

$$f_n = \frac{n \cdot u}{2 \cdot L} \qquad (2)$$

where *L* is the inner length of the cavity and *n* = 1, 2, 3, …

A dependency of the speed of sound on thermodynamic temperature *T* is well discussed in the field of acoustic gas thermometry (e.g., in [13] and [14]). The absolute AGT determines *T* from measurements of *u* in a low-density monatomic gas (of average molar mass equal to *M*). The method involves the measurement of the resonant frequencies of standing waves in cavities of simple geometry (see[15]), made of stainless steel or copper (according to[16]). As mentioned in [17], principles of AGT are related to the basic formula, relating Laplace's definition of the zero-pressure speed of sound u_0 and *T*,

This project 19ENG09 BIOFMET has received funding from the EMPIR programme co-financed by the Participating States and from the European Union's Horizon 2020 research and innovation programme.

EMPIR EURAMET
The EMPIR initiative is co-funded by the European Union's Horizon 2020 research and innovation programme and the EMPIR Participating States

$$u_0^2(T) = \frac{\gamma RT}{M}, \tag{3}$$

Where γ denotes the heat capacity ratio and R is the molar gas constant.

When measuring using the air medium, Equation (2), describing the relation between the speed of sound in an ideal gas and the thermodynamic temperature is simplified and used to compute the temperature estimation. This approximation does not take into account such effects as pressure, humidity, gas composition and others influencing the precision and limits of operation of the measurement experiment. The simplification was performed as follows:

$$u_{air} = \sqrt{\frac{\gamma RT}{M}}. \tag{4}$$

M here is expressed in g·mol^{-1} and the value of R used for measurements with air media is determined in [18]. In addition, the values of κ and M for the average air, are listed e.g., in [19]. Substituting these specific values into Equation (4), the following relationship is obtained:

$$u_{air} = 331.41 + \sqrt{1 + \frac{t}{273.15}} \tag{5}$$

When using only the first two terms of the Taylor expansion it reduces to the form of

$$u_{air} = 331.41 + 0.61 \cdot t, \tag{6}$$

where t is the temperature in °C and combining this equation with Equation (2), the influence of the temperature on resonance frequency in the air can be expressed as

$$f_n = \frac{n \cdot (331.41 + 0.61 \cdot t)}{2 \cdot L}. \tag{7}$$

The influence of humidity on wave propagation lies in the magnitude of sound energy attenuation. The complexity of the situation arises due to its dependence on T and frequency. To simplify an idea, the dependences of the attenuation coefficient for various frequencies of sound and fixed T are shown e.g., in [20]0 and (shown in Figure 13).

This project 19ENG09 BIOFMET has received funding from the EMPIR programme co-financed by the Participating States and from the European Union's Horizon 2020 research and innovation programme.

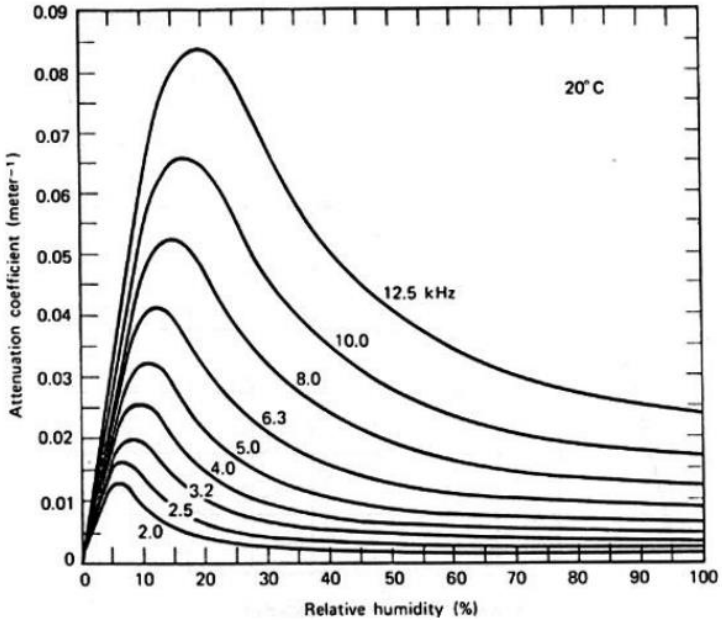

Figure 16: Relative humidity versus attenuation coefficient in m-1 at a fixed temperature (as taken from[20])

To show the full scale of possible changes caused by the change in humidity the extremes of dry air and water vapour are taken into the consideration. The density of the dry air is taken from [21] as ρ_d = 1.20479 kg/m^3 and the density of water vapour is taken from [22] as ρ_v = 0.756182 kg/m^3. The heat capacity ratio at 20 °C is 1.4 for dry air and 1.33 for water vapour [23]. From it we can infer the ratio of the speed of sound in the dry air u_d and in the water vapour u_v shows the scale of the maximum relative change caused by this effect:

$$\frac{u_d}{u_v} = \sqrt{\frac{\gamma_d}{\gamma_v}\frac{\rho_v}{\rho_d}} \cong 0.813. \qquad (8)$$

The second effect of humidity on sound propagation is attenuation. This phenomenon is used especially in room acoustics, namely in sound absorption coefficient measurement in reverberation measuring chambers where humidity is intentionally increased to decrease the sound attenuation expressed by the attenuation constant *m* [24].

The situation becomes much more complex when introducing a load into the resonator (in this case in the form of biofuel material). Dimensions of wood chips and wood pellets allow sound to propagate in the resonator even when loaded by such samples, thanks to the diffraction effect, described e.g., in [25]. Despite that the sound frequency will remain unaffected, the attenuation caused by the presence of the load is present. When the cylinder is filled with the material a sound field is expected to be similar to the case of sound

This project 19ENG09 BIOFMET has received funding from the EMPIR programme co-financed by the Participating States and from the European Union's Horizon 2020 research and innovation programme.

propagating through an extremely porous solid piece of material. Several studies on porous material can be found e.g., in [26], [27] and [28]. No study covering the general theory on sound propagation in the porous material of various moisture is available. For this reason, the experiments that can be found in articles deal only with case studies. As concluded e.g., in [29]0 the characterization of the system, focused on specific material (optimally supported by e.g., FEM modelling) must be done to find e.g., moisture-power loss transfer function.

2.2.2.2 Implementation

2.2.2.2.1 -Sample preparation and traceability

Woodchips produced by *AGRO CS a. s.* company are originally intended as a drainage layer for raised flowerbeds. It is made of natural, chemically untreated coniferous wood (of unspecified type), which is only mechanically "chipped" into small pieces. Their coarse structure with sufficient non-capillary pores ensures increased permeability to air and water. Wood pellets (of unspecified wood type) are produced by *Dřevovýroba HEPA, s.r.o* company. According to the producer, purely natural pellets are compressed under the pressure of 1220 $kg \cdot m^3$, and thus are produced completely without adhesives and chemicals. Both materials are commonly available at DIY shops and are distributed in sealed plastic bags.

Reference dry samples were prepared following the LoD method (using an automated *Chirana STE 23/1* drying oven) and subsequently stored in a common desiccator with silica gel beads. Emphasis was placed on minimizing the amount of time that samples are exposed to the surrounding atmosphere due to the hydrophilic nature of wood.

To moisten the samples, moist air, prepared at gas mixing generator (see Figure 14) was used. The principle is based on mixing dry and wet gases. The device contains two pipelines. Dry gas flows one way; thus, the gas that does not pass through the saturator, the second path is equipped with a saturator, where the gas is wetted. Both paths are connected in a mixing vessel, where the given water dew point (frost point resp.) temperature is reached by mixing these gases in a specific proportion. The mixing generator is a secondary device connected to the primary generator by a dew point meter. In addition to the saturator and mixing vessel, the saturator consists of a pressure gauge, a differential pressure gauge, thermal mass flow meters and cells with different fittings for different types of customer devices.

This project 19ENG09 BIOFMET has received funding from the EMPIR programme co-financed by the Participating States and from the European Union's Horizon 2020 research and innovation programme.

EMPIR EURAMET
The EMPIR initiative is co-funded by the European Union's Horizon 2020 research and innovation programme and the EMPIR Participating States

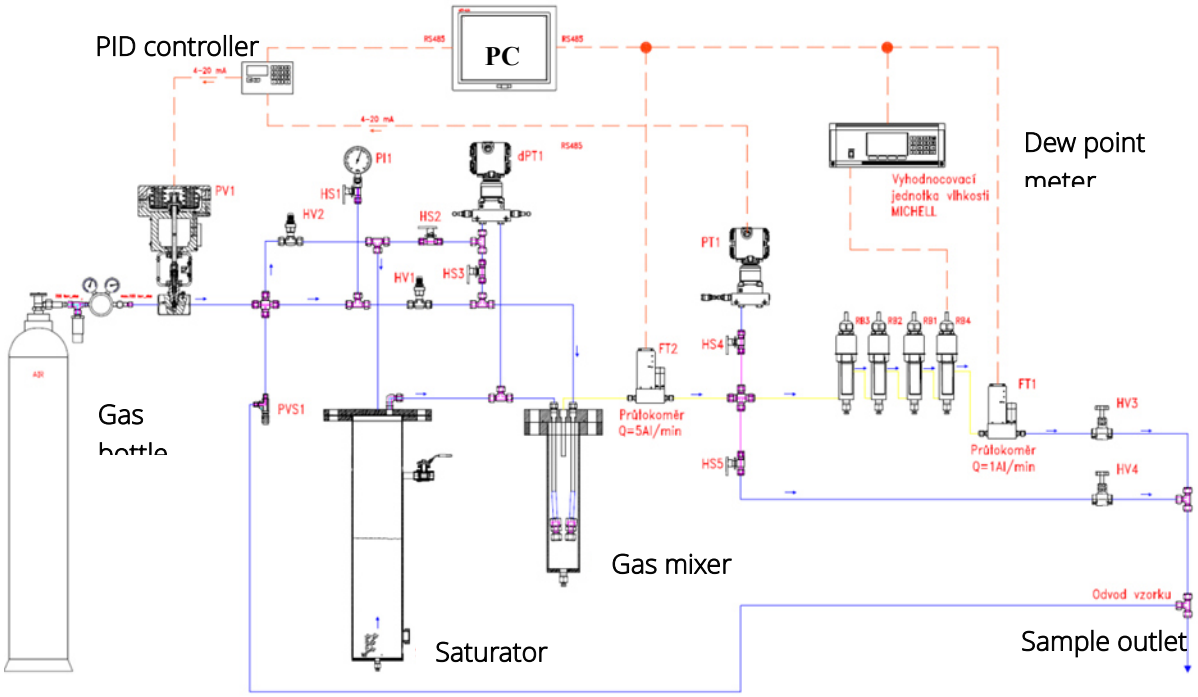

Figure 17: Principal scheme of humidity generator

The carrier synthetic air of a defined flow was flowing through a cell containing a given wooden material, that was previously subject to drying. The resulting moisture was measured by the LoD method. The time needed to obtain the necessary moisture of the sample was not known in advance and was determined experimentally during the wetting procedure by the LoD method. The SI traceability was realized to mass through the *KERN ABJ 320-4NM* calibrated analytical balance. Air temperature, humidity and atmospheric pressure were monitored by calibrated digital *COMET D 4141* thermo-hygro-barometer to follow requirements on environmental conditions, required by standards [30], [31] and [32]. The results of its water content measurement were used to characterize the transfer function of the prototypal device.

2.2.2.2.2 Resonance cavity

The cylindrical stainless-steel cavity serves as a gas-tight container for solid biofuels under test. Dimensions of the resonator are shown in Figure 15.

This project 19ENG09 BIOFMET has received funding from the EMPIR programme co-financed by the Participating States and from the European Union's Horizon 2020 research and innovation programme.

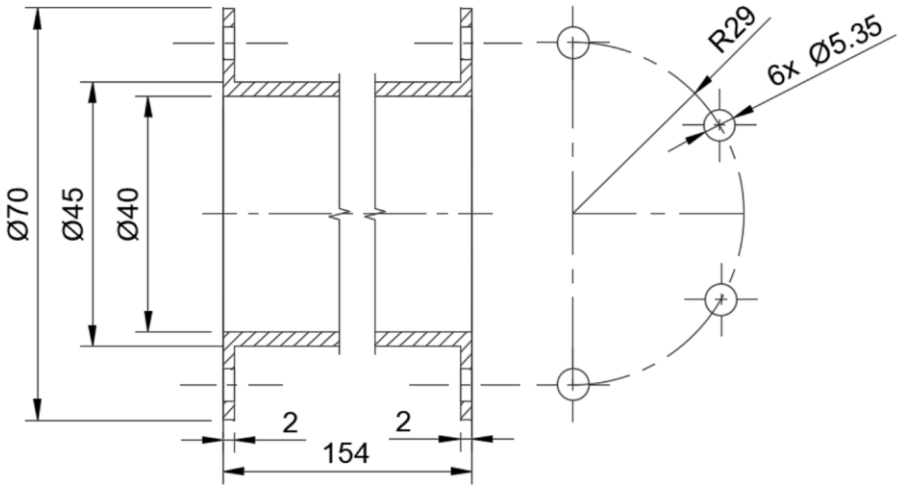

Figure 18: Sketch of the cavity, dimensions in mm

During the measurement, the cavity is closed at both ends by flat lids, using common rubber gaskets and connected to the cylinder by stainless steel bolts and nuts. Stainless steel was selected for its relatively low thermal conductivity in comparison to other affordable metals (to slow down the influence of temperature fluctuations) and durability against a harsh industrial environment.

Axial resonance modes are experienced to be of higher power magnitude than radial modes, therefore the region of interest was focused on corresponding longitudinal frequencies. Expected values of natural modal longitudinal frequencies (l = 1, ..., 5) were calculated using eq. (2) in section 2.2.2.1 above and depend on temperature (e.g., for 23 °C its values are approximately 1122 , 2243, 3365, 4486 and 5608) Hz.

2.2.2.2.3 Acoustic hygrometer

The experimental device for the determination of water content in wooden pellets and woodchips is based on measuring the power loss at several acoustic resonance modes. Several longitudinal acoustic resonance modes are excited in the cylindrical waveguide. Such a sound field arises as a result of sweeping the frequency of the waveform generator that includes eigenfrequencies of the resonance cylinder. The power at each longitudinal mode is then derived from the data record of the response from the microphone. Since the metrological traceability is performed by the LoD method (following ISO 18134-1:2015 [3], ISO 18134-2:2017 [4] and ISO 18134-3:2015 [5].) supported by calibrated balance and set of reference woodchip materials, the device described here is the secondary system. The stainless-steel cavity serves as a container for measured samples (see Figure 16). The ratio ---of power measured by an acoustic receiver at specific sample moisture to power measured

This project 19ENG09 BIOFMET has received funding from the EMPIR programme co-financed by the Participating States and from the European Union's Horizon 2020 research and innovation programme.

at a reference dry sample, at various resonance frequencies is dependent on the content of moisture in a sample.

The reported prototype can perform an estimation of average moisture by analysis of an acoustic signal following the interaction between moist woodchips (wood pellets resp.) and surrounding air in a relatively short period. The novelty of the presented work consists of a combination of several aspects: the use of acoustic resonances of air in a cylindrical resonance cavity and the use of the cavity as a container for measured samples. The method of measurement is inspired by the conclusions of several research activities focused on moisture in various wood samples and soil e.g. [6], [7], [8], [9], [10] from whose the assumption that the moisture content in wooden material affects the speed and attenuation of sound was taken into account.

Figure 19: Cavity filled by subsequently tested material

The prototype can be divided into 3 parts, providing together its function. The first part is a signal generator, together with an acoustic transducer, that creates a sound field inside the resonator. Calibrated *SIGLENT SDG1025* function/arbitrary waveform generator, controlled by the LabVIEW application, carries out production of 5 frequency swept signals of 4 V_{pp} amplitude, sweep time of 30 ms and frequency ranges around expected resonance longitudinal modes (that shift on frequency axe as a function of temperature). Common *ROCCAT ROC-14-210* headphone (with connector modified to match coaxial BNC generator output) served as an acoustic source. The principal scheme describing the measurement system can be found in Figure 17.

This project 19ENG09 BIOFMET has received funding from the EMPIR programme co-financed by the Participating States and from the European Union's Horizon 2020 research and innovation programme.

EMPIR EURAMET
The EMPIR initiative is co-funded by the European Union's Horizon 2020 research and innovation programme and the EMPIR Participating States

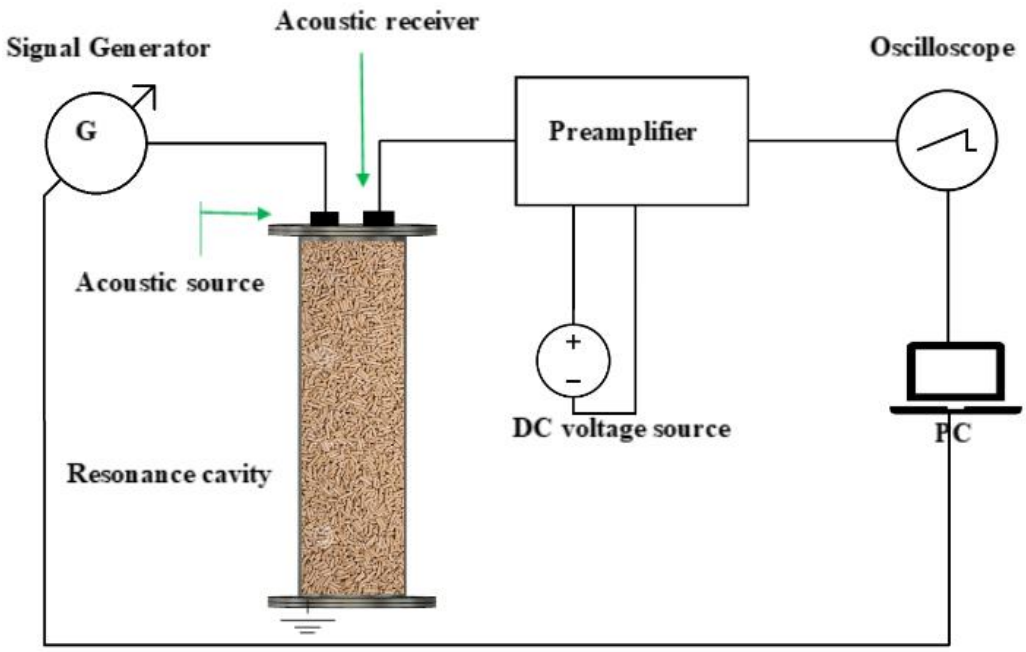

Figure 20: Scheme of the measurement system in use

The second part is responsible for the measurement of the sound inside the resonator. It includes HITPOINT PMOF 9767 NW-46DQ electret condenser microphone supported by JABEL ZSM-250 microphone preamplifier with adjustable gain. Owon ODP3032 30V/3A/195W Linear DC Power Supply serves as a stabilised supply voltage source for the preamplifier. The third part of the system is maintaining the analysis of measured data that is made in two steps. The primal analysis is carried out by the OWON SDS8302 300 MHz, 2.5 GSa/s calibrated digital oscilloscope. The second step is done in the LabVIEW environment that is operating on the common office computer. The data is transferred to a computer via a type B USB cable. The whole system is shown in Figure 18.

This project 19ENG09 BIOFMET has received funding from the EMPIR programme co-financed by the Participating States and from the European Union's Horizon 2020 research and innovation programme.

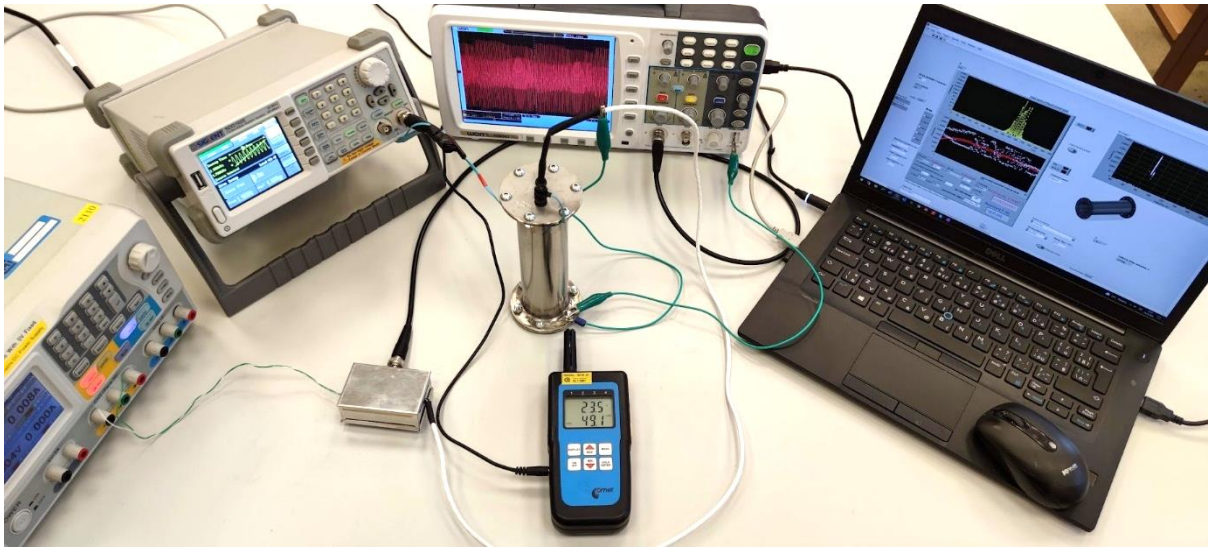

Figure 21: Measurement setup for moisture content determination as sketched in Figure 5, accompanied by thermo-hygro-barometer to monitor environmental conditions

The situation is different when calibrating the device. Two Bruel & Kjaer 4939 ¼" microphones serve to excite and record an acoustic field in the cavity. The source microphone is connected through the G.R.A.S RA0086 Transmitter Adapter and GRAS 14AA Electrostatic Actuator Amplifier to the HP 33120A function generator that also provides a reference signal for the lock-in amplifier. Receiving microphone with Bruel & Kjaer 2669 microphonic preamplifier is connected through the Bruel & Kjaer 2690-A NEXUS Conditioning Amplifier to the measuring channel of the STANFORD RESERCH SYSTEMS SR830 lock-in amplifier. This setup (Figure 19) is selected to exclude possible uncertainty connected with instruments that are employed during use of the cavity for common measurement.

This project 19ENG09 BIOFMET has received funding from the EMPIR programme co-financed by the Participating States and from the European Union's Horizon 2020 research and innovation programme.

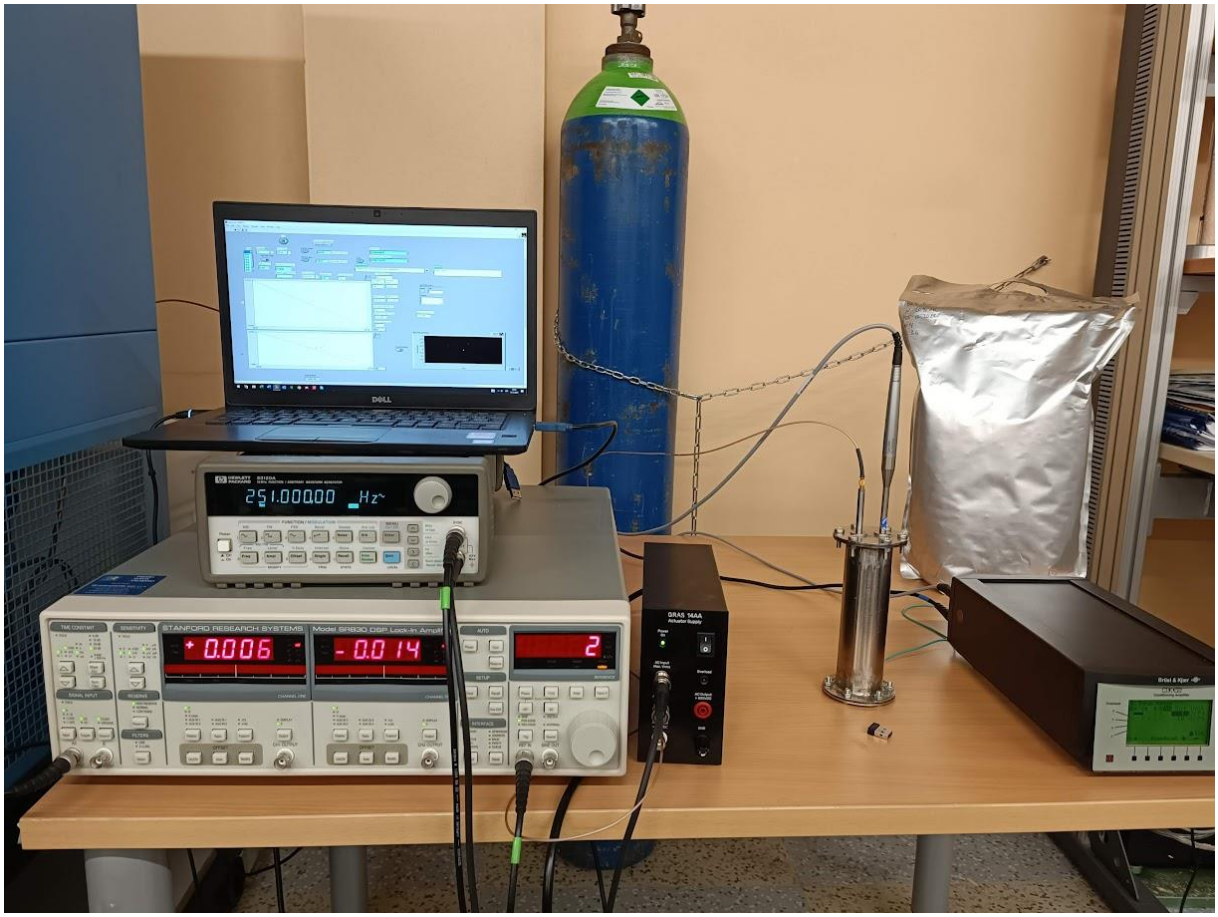

Figure 22: Measurement setup with acoustic resonance cavity to find power ratio of woodchip sample material of given moisture to reference dry woodchip material

The acoustic hygrometer needs to be calibrated for each material type separately, due to its matrix dependence. However, calibration at wood pellets was generally performed in the range from approximately 0 %mc to 10 %mc and at woodchips in the range from approximately 30 %mc to 55 %mc using the LoD method described in ISO 18134-3 standard. Additionally, reference woodchip material from DTI served to calibrate the device in the range from approximately 0 %mc to 50 %mc.

This project 19ENG09 BIOFMET has received funding from the EMPIR programme co-financed by the Participating States and from the European Union's Horizon 2020 research and innovation programme.

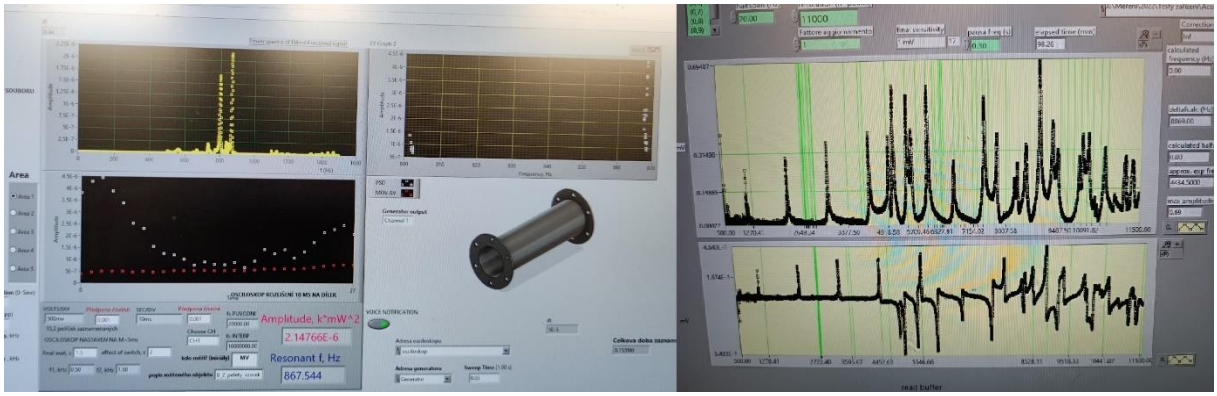

Figure 23: LabView application for common measurements (left), LabView application used for calibration of the cavity power ratios-to-moisture characteristics

Results of characterisation for two different woodpellet producers are shown in Figure 24 and Figure 25.

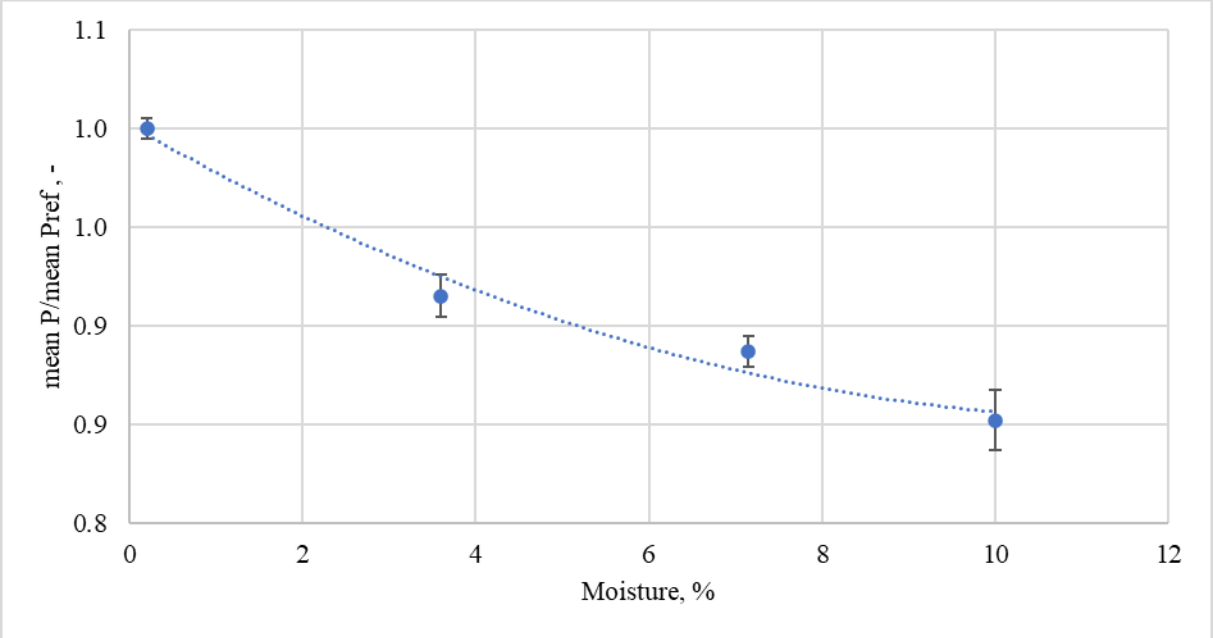

Figure 24: Results of characterisation at woodpellets, producer A

This project 19ENG09 BIOFMET has received funding from the EMPIR programme co-financed by the Participating States and from the European Union's Horizon 2020 research and innovation programme.

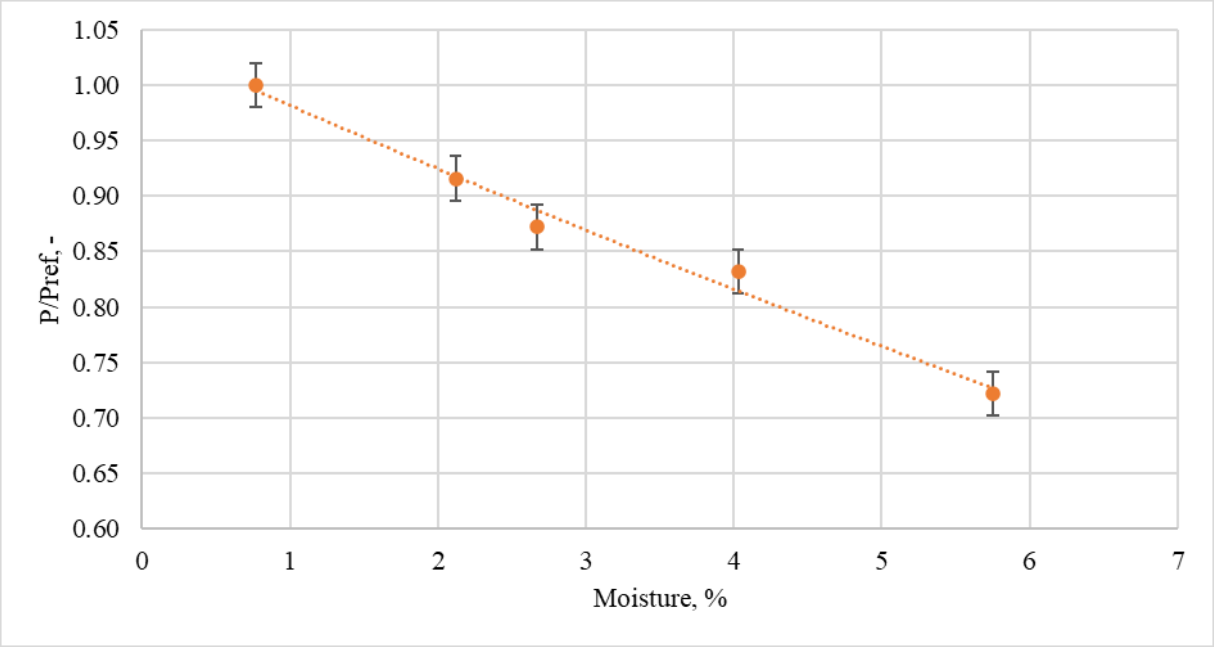

Figure 25: Results of characterisation at woodpellets, producer B

Example of woodchips measurement results are shown in Figure 26

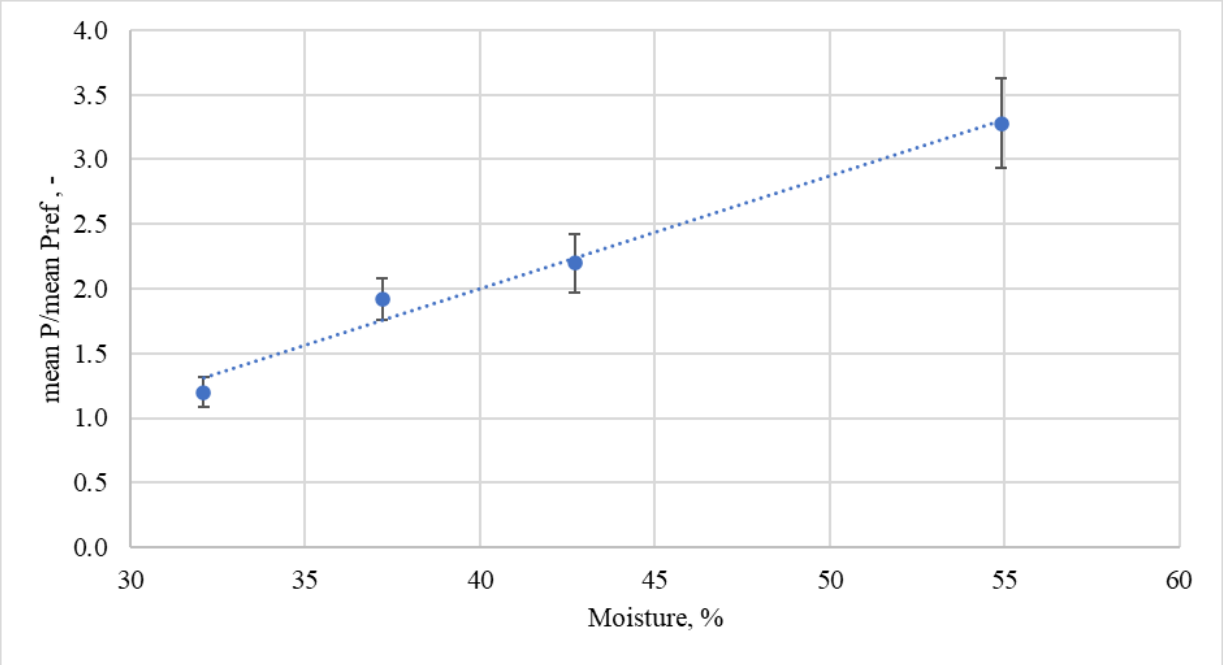

Figure 26: Measurement results for wood chips

2.3 Traceability routes

Traceability is commonly represented as a pyramid, with the reference of the SI unit at the top and the end-users who rely on daily measurements at the bottom. Between these two

This project 19ENG09 BIOFMET has received funding from the EMPIR programme co-financed by the Participating States and from the European Union's Horizon 2020 research and innovation programme.

extremes, there are various intermediate levels that play a crucial role in connecting the highest level to the end-users.

According to the International Vocabulary of Metrology, traceability is defined as the property of a measurement result that allows it to be linked to a reference through a continuous chain of calibrations. The process of transmitting this traceability from the reference to the end-users is known as dissemination.

The International Vocabulary of Metrology provides definitions for traceability, highlighting the importance of calibrations and the associated uncertainty in establishing and maintaining an unbroken chain of comparisons.

In essence, traceability relies on the accuracy and reliability of calibrations to ensure the continuity of measurements throughout the entire traceability chain, ultimately providing confidence in the reliability and comparability of measurement results for end-users.

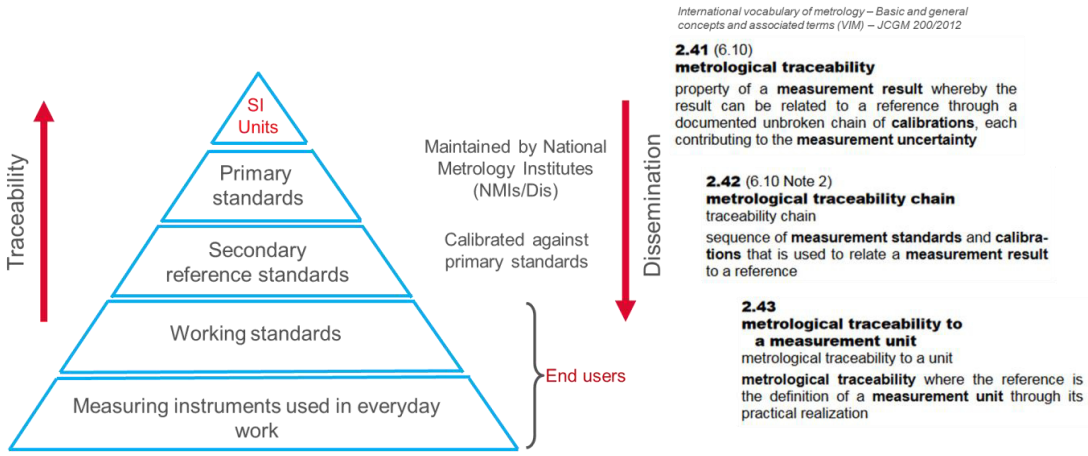

Figure 27: Schematic of traceability

Why is traceability so important? Let's consider two countries, A and B, where two companies are conducting moisture measurements on wood pellets. Each company ensures the traceability of their daily measurements through an internal metrology laboratory. These internal laboratories calibrate their standards using an external metrology laboratory, and this process continues until the reference level is reached. Thus, an unbroken chain of calibrations is maintained in each case.

This project 19ENG09 BIOFMET has received funding from the EMPIR programme co-financed by the Participating States and from the European Union's Horizon 2020 research and innovation programme.

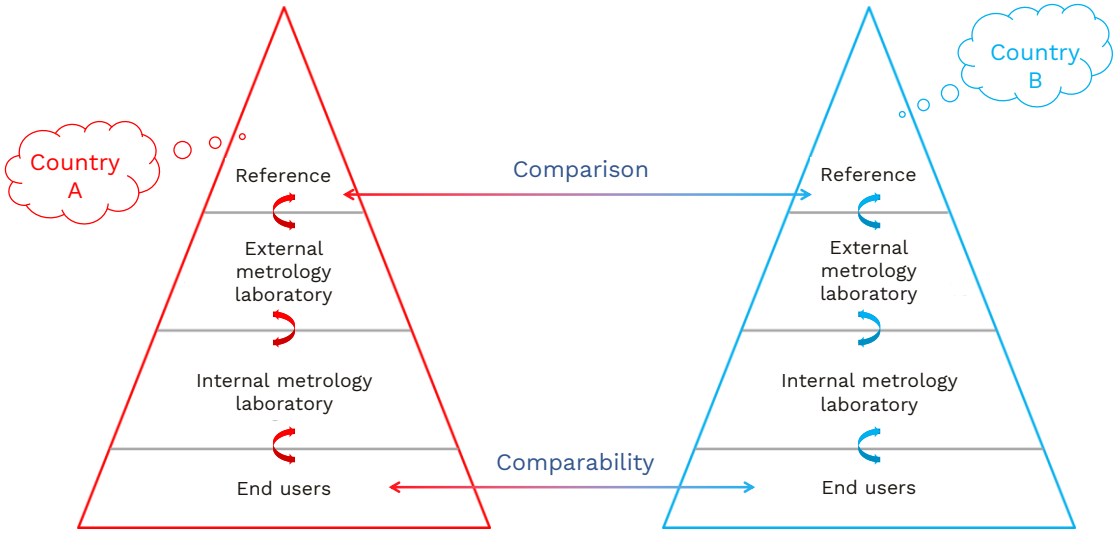

Figure 28: Schematic of traceability

At the highest level of the traceability chain, national metrology laboratories participate in inter-laboratory comparisons. These comparisons are essential to verify their calibration capabilities and associated uncertainty claims. Consequently, if the results and associated uncertainties of national metrology laboratories are compatible, and if the dissemination of traceability is ensured from the highest level down to the end-users, then the measurements performed on each side become comparable. This comparability is made possible by the traceability and coherence maintained at the highest level of the traceability chain.

In summary, traceability is crucial because it allows for the comparability of measurements across different entities and ensures that measurement results can be trusted and relied upon. By establishing an unbroken chain of calibrations and maintaining consistency in traceability at all levels, confidence in the accuracy and reliability of measurements is achieved, benefiting both companies and end-users alike.

When establishing traceability routes for an instrument or a measurand related to material properties, such as humidity content, the following possibilities can be considered:

- Primary measurement standard
    - measurement standard established using a primary reference measurement procedure, or created as an artifact, chosen by convention
    - provide traceability to SI and related uncertainty

This project 19ENG09 BIOFMET has received funding from the EMPIR programme co-financed by the Participating States and from the European Union's Horizon 2020 research and innovation programme.

Figure 29: Illustration of traceability to the International System of Units (SI) achieved by using a primary measurement standard for wood pellets or wood chips

- Secondary measurement standard
  - measurement standard established through calibration with respect to a primary measurement standard, or certified reference material, for a quantity of the same kind
  - provide traceability to SI and related uncertainty
- Certified Reference Materials (CRMs)
  - ready made sample for calibrating measuring device
  - provide traceability to SI and related uncertainty

This project 19ENG09 BIOFMET has received funding from the EMPIR programme co-financed by the Participating States and from the European Union's Horizon 2020 research and innovation programme.

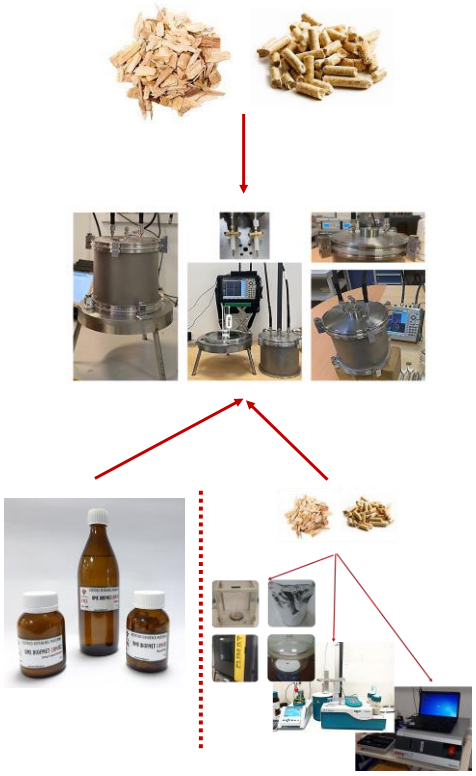

Figure 30: Illustration of traceability to the International System of Units (SI) achieved by using a secondary measurement standard calibrated with respect to a primary measurement standard or certified reference material for wood pellets or wood chips

By implementing one of the traceability schemes presented above, or by combining them, it is possible to ensure the traceability of humidity content measurements for wood pellets or wood chips using in-line or on-line instruments, as illustrated in the figure below.

Here, the calibration of the in-line or on-line instruments can be achieved by using either a calibrated secondary measurement standard or a calibrated primary measurement standard. However, in both cases, it requires the use of materials that need to be measured by the in-line or on-line instruments. This involves establishing a calibration curve between the instrument to be calibrated and the reference, using materials prepared at different moisture levels.

This project 19ENG09 BIOFMET has received funding from the EMPIR programme co-financed by the Participating States and from the European Union's Horizon 2020 research and innovation programme.

Figure 31: Illustration of traceability to the International System of Units (SI) achieved by using either a calibrated secondary measurement standard or a calibrated primary measurement standard for the measurement of humidity content in wood pellets or wood chips

3 Experimental results

Several comparisons have been made between the reference methods for evaluating their performance, measuring material moisture.

3.1 Interlaboratory Comparison

An interlaboratory comparison (ILC) was carried out between CETIAT, CMI and DTI, where both loss on drying and alternative methods were used, and tests were carried out by DTI on samples originating from a district heating plant, where the EWV + dew point hygrometer method was compared to a standard loss on drying method, performed by the biomass laboratory at DTI.

With few laboratories in the intercomparison, and all laboratories of expected equal measurement capabilities, a consensus value for the reference value is calculated. Analysis of the results show, that only CMI and the biomaterials laboratory at DTI measured values

This project 19ENG09 BIOFMET has received funding from the EMPIR programme co-financed by the Participating States and from the European Union's Horizon 2020 research and innovation programme.

consistent with the consensus value, mainly due to, that the stated uncertainty of these two laboratories was larger than what is stated for the loss on drying from CETIAT and the EWV-LoD at DTI. In the ILC, CETIAT measured moisture levels which were significantly lower than the consensus value, while DTI measured moisture values which were significantly higher than the consensus value.

A more thorough analysis shows, that the results from the two loss on drying methods performed at DTI overlap.

The biomass laboratory at DTI, who perform LoD-measurements at a much higher rate than the EWV-laboratory states an uncertainty twice as high as the EWV-LoD, and it appears, that this uncertainty is more realistic than what is found at both CETIAT and the EWV-LoD at DTI.

Results from the loss on drying analysis is seen in Figure 25

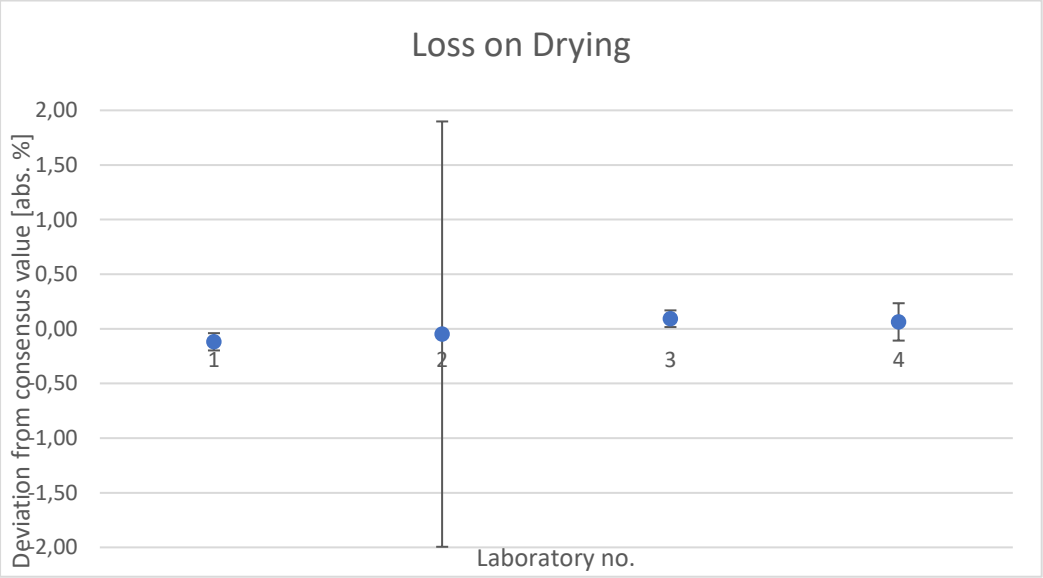

Figure 32: Measurement errors with respect to consensus value from loss on drying. Laboratory 1: CETIAT, laboratory 2: CMI, laboratory 3: DTI EWV-lab, laboratory 4: DTI Biomass-lab according to EN 14774-2.

A similar analysis, comparing measurement results of material moisture is performed between the non-loss on drying methods conducted by CETIAT, CMI, and DTI. Here, only the DTI EWV-lab participated, as the DTI biomass laboratory only has facilities to perform loss on drying.

The results from this intercomparison are seen in Figure 26.

Here it is seen, that there is a high level of agreement between the three laboratories, and despite the stated uncertainty of CETIAT and DTI being significantly lower than the

This project 19ENG09 BIOFMET has received funding from the EMPIR programme co-financed by the Participating States and from the European Union's Horizon 2020 research and innovation programme.

uncertainty from CMI, they still have overlapping results. In the loss on drying method, both CMI and DTI have stated uncertainties at around 0.05 % moisture content, while for the non-LoD, their stated uncertainties are twice as high at 0.1 % moisture content. The results could indicate, that the stated uncertainty on the LoD from CETIAT and DTI's EWV-LoD should be at the same level as the stated uncertainties from their primary standards.

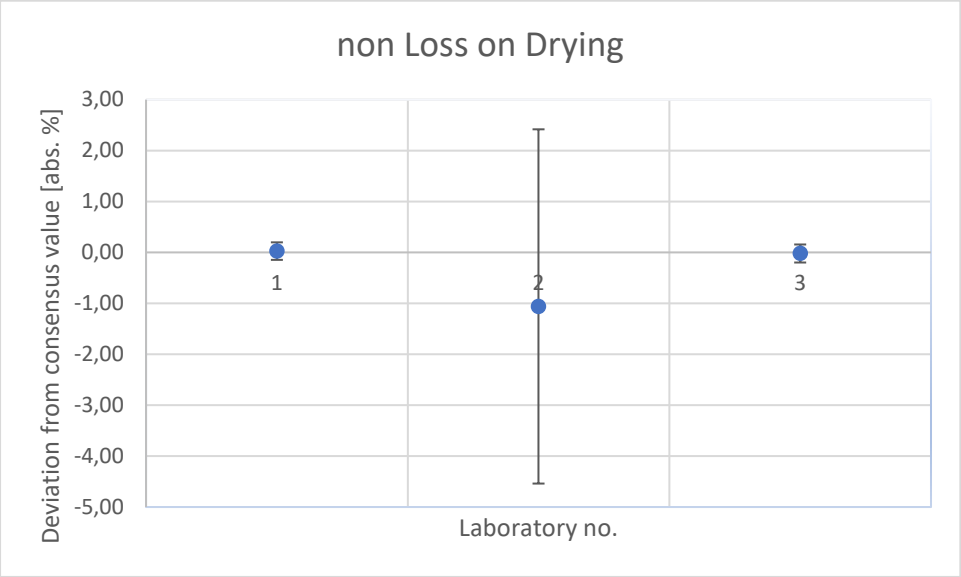

Figure 33: Measurement errors with respect to consensus value from non-loss on drying. Laboratory 1: CETIAT EWV (thermo-coulometry), laboratory 2: CMI, laboratory 3: DTI EWV-Dewpoint.

3.2 Expanded analysis of DTI's EWV method

A more thorough comparison between the DTI EWV method, the EWV-LoD, and the standard loss on drying method, also conducted at DTI is performed using wood chips

The wood chips are of high quality, and prepared to have different moisture levels, to allow analysis over a wide range.

10 kg of samples are prepared for 12 different moisture levels, although including one empty bin (to get a 0-level reading). Furthermore, data from one of the moisture levels were excluded from the analysis, due to inconsistent measurement results, where a repetition of the loss on drying gave significantly different results.

Data from this analysis is seen in Figure 33. For all the measurements, there is a good consistency between the EWV results and the EWV-LoD.

There seems to be some inconsistencies between the EWV/EWV-LoD and the standard LoD at above 30 % moisture content. For the majority of measurements, the EWV/EWV-LoD show higher moisture content than the standard loss on drying method.

This project 19ENG09 BIOFMET has received funding from the EMPIR programme co-financed by the Participating States and from the European Union's Horizon 2020 research and innovation programme.

Since the EWV and the EWV-LoD are consistent with each other, this could go to indicate, that the signal used to stop the drying process used in the EWV (stop the drying, when the measured dew point gets below -15 °C), allows for a higher degree of drying than the standard LoD. Given that a standard LoD is taking place in an oven using ambient air, having a dew point significantly higher than -15 °C, this does not seem unreasonable. That the effect is not seen at lower moisture contents, can most likely be caused by the measurement uncertainty of the setup.

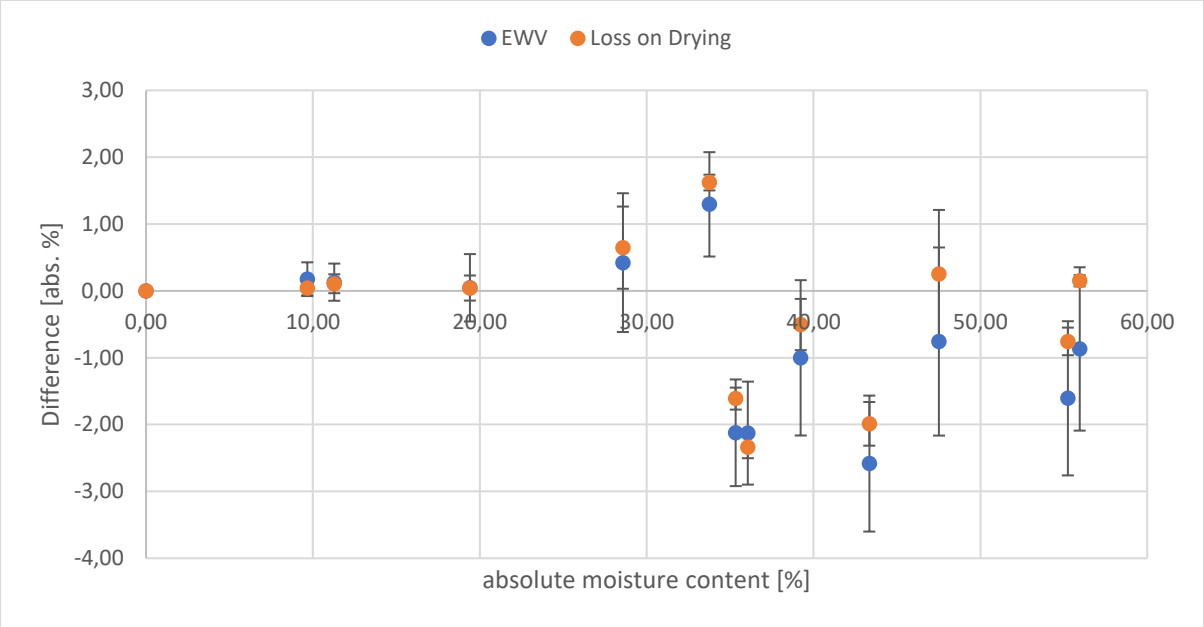

Figure 34: Comparison of the DTI EWV method and simultaneous loss on drying with a standard loss on drying

The results of the measurements are seen in Figure 27.

Although significant differences between EWV and loss on drying are seen in the analysis, most of the results indicate that there is a high level of agreement between the two methods. This is valuable information, as loss on drying is used significantly more than the EWV + dew point hygrometer method. The results from this comparison thus indicate, that the loss on drying can be used to obtain valid results, as long as the uncertainty of the results are evaluated, not just on the basis of the resolution of the scale, but also taking other factors into account.

This project 19ENG09 BIOFMET has received funding from the EMPIR programme co-financed by the Participating States and from the European Union's Horizon 2020 research and innovation programme.

4 Conclusion

In this report, we have presented the reference methods utilized within the BiofMET project for measuring the humidity content, specifically moisture content or water content. Each reference method, including loss on drying, oven coulometric Karl Fischer titration, evolved water vapor coulometric Karl Fischer titration, evolved water vapor coulometric analysis, and evolved water vapor dew-point analysis, has been described, and the main sources of uncertainty have been outlined.

In addition to the reference methods, two transfer standards have been developed: an electromagnetic resonant cavity and an acoustic resonant cavity. The electromagnetic resonant cavity relies on the perturbation induced on the resonance frequency when the cavity is filled with the material to be measured. On the other hand, the acoustic resonant cavity is based on the influence of humidity on the propagation of waves and the attenuation of sound energy.

With the implementation of the reference methods in the laboratory of the JRP partners, the calibration of each transfer standard can be ensured. We have highlighted the various traceability schemes that guarantee traceability to the International System of Units (SI). These traceability schemes can be applied to both in-line or on-line instruments or directly to the measurand of interest, which is the moisture content or water content of wood pellets or wood chips.

Finally, we have presented a comparison that demonstrates the paramount importance of the traceability scheme, as it validates the reliability and coherence of the primary reference methods. These methods serve as the foundation for disseminating traceability to end-users, ensuring the accuracy and consistency of humidity content measurements throughout the entire process.

Disclaimer:

Certain commercial equipment, instruments, and materials are identified in this report to specify adequately the experimental procedure. In no case does such identification imply recommendation or endorsement by the authors, nor does it imply that the material or equipment is necessarily the best available for the purpose.

This project 19ENG09 BIOFMET has received funding from the EMPIR programme co-financed by the Participating States and from the European Union's Horizon 2020 research and innovation programme.

The EMPIR initiative is co-funded by the European Union's Horizon 2020 research and innovation programme and the EMPIR Participating States

Appendix 1: Uncertainty budget for EVW – Dew point hygrometer

Parameter	Unit												
Temperature of LFE	°C	23	23	23	23	23	23	23	23	23	23	23	23
Temperature of chamber	°C	80	120	80	120	80	120	80	120	80	120	80	120
Dew point temperature	°C	30	30	50	50	30	30	50	50	30	30	50	50
Gauge pressure	mBar	30	30	30	30	30	30	30	30	30	30	30	30
Pressure at dew point meter	Pa	101325	101325	101325	101325	101325	101325	101325	101325	101325	101325	101325	101325
Differential pressure accross LFE	Pa	45	45	45	45	75	75	75	75	100	100	100	100
Gas flow	l/min	0.9000	0.9000	0.9000	0.9000	1.5000	1.5000	1.5000	1.5000	2.0000	2.0000	2.0000	2.0000
u(gas flow)	l/min	0.0034	0.0034	0.0034	0.0034	0.0034	0.0034	0.0034	0.0034	0.0034	0.0034	0.0034	0.0034
relative gas viscosity	-	1.014294	1.014294	1.014294	1.014294	1.014294	1.014294	1.014294	1.014294	1.014294	1.014294	1.014294	1.014294
u(relative gas viscosity)	-	0.000070	0.000070	0.000070	0.000070	0.000070	0.000070	0.000070	0.000070	0.000070	0.000070	0.000070	0.000070
Viscocity-adjusted gas flow	l/min	0.9129	0.9129	0.9129	0.9129	1.5214	1.5214	1.5214	1.5214	2.0286	2.0286	2.0286	2.0286
u(viscocity-adjusted gas flow)	l/min	0.0034	0.0034	0.0034	0.0034	0.0034	0.0034	0.0034	0.0034	0.0034	0.0034	0.0034	0.0034
Gas pressure at LFE	Pa	104325	104325	104325	104325	104325	104325	104325	104325	104325	104325	104325	104325
u(gas pressure at LFE)	Pa	100	100	100	100	100	100	100	100	100	100	100	100
Gas flow in chamber	l/min	1.0886	1.2119	1.0886	1.2119	1.8143	2.0198	1.8143	2.0198	2.4190	2.6930	2.4190	2.6930
u(gas flow in chamber)	l/min	0.0041	0.0045	0.0041	0.0045	0.0041	0.0045	0.0041	0.0045	0.0041	0.0045	0.0041	0.0045
Water vapour pressure	Pa	4247	4247	12353	12353	4247	4247	12353	12353	4247	4247	12353	12353
u(water vapour pressure)	Pa	32	32	82	82	32	32	82	82	32	32	82	82
Saturation water vapour pressure in chamber	Pa	4373	4373	12718	12718	4373	4373	12718	12718	4373	4373	12718	12718
u(Saturation water vapour pressure in chamber)	Pa	34	34	86	86	34	34	86	86	34	34	86	86
Dew point temperature, chamber	°C	30.51	30.51	50.59	50.59	30.51	30.51	50.59	50.59	30.51	30.51	50.59	50.59
u(dew point temperature, chamber)	°C	0.14	0.14	0.14	0.14	0.14	0.14	0.14	0.14	0.14	0.14	0.14	0.14
enhancement factor, chamber	-												
alpha	-	0.001736	0.001736	0.003618	0.003618	0.001736	0.001736	0.003618	0.003618	0.001736	0.001736	0.003618	0.003618
u(alpha)	-	0.000009	0.000009	0.000017	0.000017	0.000009	0.000009	0.000017	0.000017	0.000009	0.000009	0.000017	0.000017
beta	-	0.0001178	0.0001178	0.0002960	0.0002960	0.0001178	0.0001178	0.0002960	0.0002960	0.0001178	0.0001178	0.0002960	0.0002960
u(beta)	-	0.0000008	0.0000008	0.0000017	0.0000017	0.0000008	0.0000008	0.0000017	0.0000017	0.0000008	0.0000008	0.0000017	0.0000017
f	-	1.004365	1.004365	1.005323	1.005323	1.004365	1.004365	1.005323	1.005323	1.004365	1.004365	1.005323	1.005323
u(f)	-	0.000030	0.000030	0.000027	0.000027	0.000030	0.000030	0.000027	0.000027	0.000030	0.000030	0.000027	0.000027
enhanced water vapour pressure	Pa	4392	4392	12786	12786	4392	4392	12786	12786	4392	4392	12786	12786
u(enhanced water vapour pressure)	Pa	34	34	86	86	34	34	86	86	34	34	86	86
Water gas flow, chamber	l/min	1.1364	1.2651	1.2406	1.3811	1.8940	2.1085	2.0677	2.3019	2.5253	2.8114	2.7569	3.0692
u(Water gas flow, chamber)	l/min	0.0043	0.0047	0.0047	0.0053	0.0043	0.0047	0.0047	0.0053	0.0043	0.0048	0.0047	0.0053
Absolute humidity	g/m^3	26.95	24.20	78.45	70.47	26.95	24.20	78.45	70.47	26.95	24.20	78.45	70.47
u(absolute humidity)	g/m^3	0.21	0.19	0.53	0.48	0.21	0.19	0.53	0.48	0.21	0.19	0.53	0.48
Water content/hour	g/h	30.6	30.6	97.3	97.3	51.0	51.0	162.2	162.2	68.0	68.0	216.3	216.3
u(water content/hour)	g/h	0.3	0.3	0.8	0.8	0.4	0.4	1.2	1.2	0.5	0.5	1.5	1.5
normalized uncertainty	-	0.9%	0.9%	0.8%	0.8%	0.8%	0.8%	0.7%	0.7%	0.8%	0.8%	0.7%	0.7%
normalized uncertainty (k=2)	-	1.7%	1.7%	1.5%	1.5%	1.6%	1.6%	1.4%	1.4%	1.6%	1.6%	1.4%	1.4%

This project 19ENG09 BIOFMET has received funding from the EMPIR programme
co-financed by the Participating States and from the European Union's Horizon 2020 research and innovation programme.

The EMPIR initiative is co-funded by the European Union's Horizon 2020 research and innovation programme and the EMPIR Participating States

5 Bibliography

[1] R. Aro, "Implementation of primary methods for the measurement of moisture content in solids", master's thesis, Aug. 2017

[2] A. L. D. D'adrian, "Method of and means for preventing sweating of glass of refrigerating cases and the like," US1913702 (A), 13-Jun-1933.

[3] F. A. Keidel, "Apparatus for water determination," US2830945 (A), 15-Apr-1958.

[4] C. E. Berry, "Electrolytic cell," US2993853 (A), 25-Jul-1961.

[5] R. Aro, "Moisture in Solids: Comparison Between Evolved Water Vapor and Vaporization Coulometric Karl Fischer Methods", International Journal of Thermophysics (2020) 41:113

https://doi.org/10.1007/s10765-020-02697-6

[6] K. Fischer, "A new method for the volumetric determination of the water content of liquids and solids," Angew. Chem., vol. 48, pp. 394–396, 1935.

[7] "One-Component Reagents for Volumetric Karl Fischer Titration," Sigma-Aldrich. [Online]. Available: http://www.sigmaaldrich.com/technical-documents/articles/analytical/karl-fischer-titration/volumetric-reagents/one-component.html. [Accessed: 06-Jun-2017]

[8] P. Bruttel and R. Schlink, "Water Determination by Karl Fischer Titration." Metrohm Ltd., 2006.

[9] Hardy, B. (1998). "ITS-90 FORMULATIONS FOR VAPOR PRESSURE, FROSTPOINT TEMPERATURE, DEWPOINT TEMPERATURE, AND ENHANCEMENT FACTORS IN THE RANGE –100 TO +100 °C" The Proceedings of the Third International Symposium on Humidity & Moisture, April, 1–8 1998.

[10] Østergaard, P & Nielsen, J; "SI-Traceable water content measurements in Solids, bulks, and powders"; International Journal of Thermophysics (2018), 1-13, 39(1); DOI: 10.1007/s10765-017-2325-4

[11] Rona, A. (2007). The Acoustic Resonance of Rectangular and Cylindrical Cavities. Journal of Algorithms & Computational Technology, 1(3). https://doi.org/10.1260/174830107782424110

[12] Wang, C., & Lai, J. C. S. (2000). Prediction of natural frequencies of finite length circular cylindrical shells. Applied Acoustics, 59(4). https://doi.org/10.1016/S0003-682X(99)00039-0

This project 19ENG09 BIOFMET has received funding from the EMPIR programme co-financed by the Participating States and from the European Union's Horizon 2020 research and innovation programme.

[13] Feng, X. J., Zhang, J. T., Lin, H., Gillis, K. A., Mehl, J. B., Moldover, M. R., Zhang, K., & Duan, Y. N. (2017). Determination of the Boltzmann constant with cylindrical acoustic gas thermometry: new and previous results combined. Metrologia, 54(5), 748–762. https://doi.org/10.1088/1681-7575/aa7b4a

[14] Moldover, M. R., Gavioso, R. M., Mehl, J. B., Pitre, L., de Podesta, M., & Zhang, J. T. (2014). Acoustic gas thermometry. Metrologia, 51(1), R1–R19. https://doi.org/10.1088/0026-1394/51/1/R1

[15] Pitre, L., Sparasci, F., Truong, D., Guillou, A., Risegari, L., & Himbert, M. E. (2011). Determination of the Boltzmann constant using a quasi-spherical acoustic resonator. Philosophical Transactions of the Royal Society A: Mathematical, Physical and Engineering Sciences, 369(1953), 4014–4027. https://doi.org/10.1098/rsta.2011.0197

[16] Gavioso, R. M., Benedetto, G., Albo, P. A. G., Ripa, D. M., Merlone, A., Guianvarc'h, C., … Cuccaro, R. (2010). A determination of the Boltzmann constant from speed of sound measurements in helium at a single thermodynamic state. Metrologia, 47(4), 387–409. https://doi.org/10.1088/0026-1394/47/4/005

[17] Benedetto, G., Gavioso, R. M., Spagnolo, R., Marcarino, P., & Merlone, A. (2004). Acoustic measurements of the thermodynamic temperature between the triple point of mercury and 380 K. Metrologia, 41(1), 74–98. https://doi.org/10.1088/0026-1394/41/1/011

[18] Mohr PJ, Newell DB, Taylor BN. CODATA recommended values of the fundamental physical constants: 2014. Rev Mod Phys 2016;88:035009. doi:10.1103/RevModPhys.88.035009.

[19] Fatihah N. and coll., PROPERTY TABLES AND CHARTS (SI UNITS) n.d., https://www.academia.edu/4637146/PROPERTY_TABLES_AND_CHARTS_SI_UNITS

[20] Bohn, D. A. (1987). Environmental Effects on the Speed of Sound. Audio Engineering Society. http://www.aes.org/e-lib/browse.cfm?elib=4916

[21] Composition of AIR, DRY (NEAR SEA LEVEL). (n.d.). Retrieved May 25, 2022, from https://physics.nist.gov/cgi-bin/Star/compos.pl?ap104

[22] Composition of WATER VAPOR. (n.d.). Retrieved May 25, 2022, from https://physics.nist.gov/cgi-bin/Star/compos.pl?refer=ap&matno=277

This project 19ENG09 BIOFMET has received funding from the EMPIR programme co-financed by the Participating States and from the European Union's Horizon 2020 research and innovation programme.

[23] White, Frank M. (October 1998). Fluid Mechanics (4th ed.). New York: McGraw Hill. ISBN 978-0-07-228192-7

[24] Kuttruff, H.: Room Acoustics, 5th edition, Spon Press, 2009 and Beranek, L.L. (1960), Noise Control, McGraw-Hill, New York

[25] Kawai, T. (1981). Sound diffraction by a many-sided barrier or pillar. Journal of Sound and Vibration, 79(2), 229–242. https://doi.org/10.1016/0022-460X(81)90370-9

[26] Li, X., Liu, B., & Wu, Q. (2022). Enhanced Low-Frequency Sound Absorption of a Porous Layer Mosaicked with Perforated Resonator. Polymers, 14(2). https://doi.org/10.3390/polym14020223

[27] Yang, T., Hu, L., Xiong, X., Petrů, M., Noman, M. T., Mishra, R., & Militký, J. (2020). Sound absorption properties of natural fibers: A review. In Sustainability (Switzerland) (Vol. 12, Issue 20). https://doi.org/10.3390/su12208477

[28] Horoshenkov, K. v., & Jaouen, L. (2013). Introduction to the special issue on acoustics of porous media. The Journal of the Acoustical Society of America, 134(6). https://doi.org/10.1121/1.4828976

[29] Pel, L., & Erich, B. (n.d.). MOISTURE CONTENT MEASUREMENT OF POROUS MATERIALS. http://www.porousmedia.nl/nfcmr/college/Vochtmeten.pdf

[30] ISO. (2015). ISO 18134-1:2015 Solid biofuels -- Determination of moisture content -- Oven dry method -- Part 1: Total moisture -- Reference method. Pub-ISO, 1.

[31] DIN. (2017). ISO 18134-2:2017 Solid biofuels -- Determination of moisture content -- Oven dry method. Pub-ISO, 2

[32] BSI. (2015). BS EN ISO 18134-3:2015; Solid biofuels - Determination of moisture content - Oven dry method - Part 3: Moisture in general analysis sample. BSI Standards Publication.

This project 19ENG09 BIOFMET has received funding from the EMPIR programme co-financed by the Participating States and from the European Union's Horizon 2020 research and innovation programme.

The EMPIR initiative is co-funded by the European Union's Horizon 2020 research and innovation programme and the EMPIR Participating States